A space–time-energy flow-based integer programming model to design and operate a regional shared automated electric vehicle (SAEV) system and corresponding charging network

Santos, Gonçalo Gonçalves Duarte; Birolini, Sebastian ; Correia , Gonçalo Homem de Almeida

DOI
10.1016/j.trc.2022.103997

Publication date
2023

Document Version
Final published version

Published in
Transportation Research Part C: Emerging Technologies

Transportation Research Part C 147 (2023) 103997

Contents lists available at ScienceDirect

Transportation Research Part C

journal homepage: www.elsevier.com/locate/trc

A space–time-energy flow-based integer programming model to design and operate a regional shared automated electric vehicle (SAEV) system and corresponding charging network

Gonçalo Gonçalves Duarte Santos [a,*], Sebastian Birolini [b], Gonçalo Homem de Almeida Correia [c]

[a] University of Coimbra, CITTA, Department of Civil Engineering, Rua Luís Reis Santos, 3030-788 Coimbra, Portugal
[b] Department of Management, Information and Production Engineering, University of Bergamo, Dalmine, BG 24044, Italy
[c] Department of Transport & Planning, Delft University of Technology, Stevinweg 1, 2628 CN Delft, the Netherlands

ARTICLE INFO

Keywords:
Integer programming
Flow-based model
Shared automated electric vehicles
Electric charging
Mathematical optimization

ABSTRACT

Shared automated vehicles are expected to be part of the supply of transportation systems in the future. Parallel to this evolution, there is the rapid penetration of battery electric vehicles (BEVs). The limitations in battery capacity and charging speed of BEVs can influence the planning and operation of shared automated electric vehicle (SAEV) systems. The design of such systems needs to include these limitations so that their viability is properly estimated. In this paper, we develop a space–time-energy flow-based integer programming (IP) model in support of the strategic design of a regional SAEV system. The proposed approach optimizes the fleet (size and composition) and charging facilities (number and location), while explicitly accounting for vehicle operations in aggregated terms (including movements with users, relocations, and charging times). The model is used to assess the impact of vehicle range and different types of chargers in the optimal design of an interurban SAEV transport system in the center of Portugal. Results show a reduction in profit as the vehicle range increases. In regards to energy, it is observed that the adoption of long-range vehicles reduces the energy spent in relocations, and increases the amount of energy charged at a lower price. Additionally, it is found that a system with long-range vehicles does not take advantage of having fast chargers. Concerning the chargers' optimal location, systems using short-range vehicles have more chargers close to the main commuter trips attracting cities, while systems with long-range vehicles have the chargers nearby the homes of users.

1. Introduction

Self-driving vehicles, also known as automated vehicles, are expected to be part of urban transportation systems in the next decades (Nieuwenhuijsen et al., 2018). This technology has several advantages, namely improving non-drivers' mobility and enhancing road safety. Services providing on-demand rides through the use of driverless vehicles are named shared automated vehicle (SAV) systems. SAV systems are potentially cheaper to run than systems with conventional vehicles in traditional on-demand services. The use of

* Corresponding author.
E-mail address: gdsantos@uc.pt (G. Gonçalves Duarte Santos).

https://doi.org/10.1016/j.trc.2022.103997
Received 23 September 2021; Received in revised form 12 October 2022; Accepted 20 December 2022

automated vehicles lowers driving costs (when compared to ride-sourcing), relocation costs (when compared to carsharing), and insurance premiums due to the reduction of accidents resulting from human error. This has the potential to reduce the service price while providing high-quality door-to-door services. These benefits should not only be associated with applications in urban areas (Imhof et al., 2020) since they may also improve the availability and quality of public transport in less dense areas (lower demand) currently with low accessibility by other means than private transport (Santos and Correia, 2021). The replacement of a low-frequency transport service performed by buses, which covers several stops in a non-direct route, with an on-demand service that uses smaller driverless vehicles and faster routes would potentially reconnect these less dense areas to the wider community. Such improvements in interurban mobility can potentially benefit local economies, making rural areas and smaller cities more attractive to visitors and future residents (Bernhart et al., 2018). The market for SAV services is expected to reach 38.61 billion dollars by 2030 (AMR, 2021). Currently, government regulations are still lagging behind when compared to the technology evolution. The only European country with legislation for the use of autonomous vehicles to provide on-demand services is Germany, with a new law approved by the Parliament in 2021 (Ewing, 2021). In the USA, a few states have already legislation that allows the operation of this type of services (Carolina, 2020), with one already available to the general public in Phoenix, Arizona (Waymo, 2022).

Parallel to the evolution of self-driving vehicles, we have been observing a fast market penetration of battery electric vehicles (BEVs) (Hao et al., 2020). Electric-powered engines are more efficient than combustion engines, although the use of batteries still has limitations in terms of vehicle range (influenced by battery capacity, charging speeds, driving conditions and weather), and ecological footprint (Wen et al., 2020). There are good chances that SAV systems will use BEV technology at the moment that fully automated vehicles become available (Taiebat and Xu, 2019). If this is the case, battery capacity and charging speed will affect the operations of shared automated electric vehicle (SAEV) systems, influencing their planning and operations (Liang et al., 2016; Scheltes and de Almeida Correia, 2017; Chen et al., 2018; Jamshidi et al., 2021). Managing the vehicles' activities between transporting clients, charging, or proactively relocating is a challenge for the upcoming SAEV systems. This management is highly dependent on the vehicle fleet, as well as on the number of charging stations (sockets) and respective charging speeds.

The design of the main system parameters of a SAEV system can essentially be done through two processes: optimization and simulation. In optimization, a model is defined based on one or more objectives to search for an optimal configuration of the system. Since the focus is on exploring the solution space as comprehensively as possible it requires a model formulation, typically in mathematical programming, that can be solved efficiently, which is not always possible. Model size and non-linearity are usually the greatest obstacles in modeling the problem of maximizing or minimizing a function in reasonable time. The simulation alternative aims to replicate the real system in the most realistic way attainable. It is possible to add several stochastic components such as demand and travel time variations and there are virtually no limitations in model components (Martinez et al., 2015). Nevertheless, as the model grows, so it does the difficulty of defining the inputs and interpreting the outputs. This approach hardly allows investigating an optimal configuration of the system, while it suitably supports the testing of different scenarios (Bierlaire, 2015). For some parameters like the fleet size, it is possible though to vary them systematically and find the value for which a certain objective function is maximized or minimized (Winter et al., 2016) but this can seldomly be studied together with other parameters.

Only a few papers have dealt with the integrated design of SAEV systems. On the optimization side, Liang et al. (2016) proposed a mathematical model to design the service area and the fleet size of a SAEV system servicing first and last-mile trips for a train station. Their model greatly simplifies the charging of the vehicles by considering an average battery whose level is based on the difference between the full battery range and the average distance travelled per vehicle (obtained from the distance traveled by all vehicles). Zhang et al. (2016) used vehicle routing with model predictive control (MPC) to optimize the movements with charging constraints. This approach was later updated by Iacobucci et al. (2019) to incorporate electricity price information for optimizing vehicle charging. The authors proposed an optimization model to jointly decide on charging (including vehicle-to-grid considerations), relocation and the routing of the vehicles. Their mixed-integer program (MIP) was tested in the case study city of Tokyo. The model does not include the location of the charging stations and it does become harder to solve for bigger instances. Both the original (Zhang et al., 2016) and the updated (Iacobucci et al., 2019) methodologies only provide optimized operation orders (transport passenger, relocate or charge), and do not design the main system parameters (fleet size, charging stations). Chen et al. (2018) proposed a routing and charging model for a small electric vehicle fleet for on-demand transit. The authors proposed a mixed-integer quadratic programming model that allows exploring the potential impact of these fleets on electric power grids. However, it does not design any component of the system as it rather focuses on the vehicle movements, including routing and charging. Huang et al. (2020) revisited the problem of the location of one-way carsharing stations but adding the electric vehicle charging constraints. Due to the difficulty in modeling each vehicle energy individually, the authors simplified the charge of the vehicles stopped at each station as a distribution that changes its shape as vehicles are picked up and returned to the different stations. The proposed methodology designs the fleet and vehicle movements (including relocations), assuming that every parking space has a charger. Jamshidi et al. (2021) have proposed a sequential mixed-integer linear programming approach for deciding in real-time when to charge electric taxis with an application in Barcelona, Spain. The model uses different temporal levels where existing data on charging requests from a whole day can help steer the real-time solutions into what is best for the system in terms of demand satisfaction. In the model, the location of charging stations is given. This approach only provides vehicle movement plans, taking the fleet and charging infrastructure as given parameters.

On the simulation side, Chen et al. (2016) used an agent-based model to simulate the operations of a fleet of SAEVs and showed that the fleet size is highly dependent on the charging infrastructure and vehicle range. This approach uses a warm-up period to generate fleet vehicles and charging stations and then implements 50 simulation runs on consecutive days to obtain the performance metrics. The conclusions are built upon admissible solutions obtained by testing five different scenarios, varying the vehicle range and charging speed. This model was later updated by Farhan and Chen (2018) to consider ridesharing with an integrated optimization and discrete event simulation framework. Similar to what was done in the previous work, this approach uses a warm-up period to define the fleet

size and the number of charging stations. It was tested for eight different scenarios varying not only the vehicle range and charging speed, but also the vehicle seating capacity. However, these works do not include a systematic search for optimal design parameters. Scheltes and Correia (2017) developed an agent-based model for simulating first/last mile connections to train stations with SAEVs. The authors model the energy of each vehicle as a function of the vehicle dynamics and test the difference between slow charging and inductive charging points scattered around the operational area. More recently the same methodology was applied in another first/last mile context linking the agent-based model to an aggregated demand model of the city of Rotterdam (Stevens et al., 2022). In both applications the fleet size is a parameter and the authors did not assess the location of chargers (small operational area). Iacobucci et al. (2018) developed a simulation methodology using a heuristic-based charging strategy to evaluate a SAEV fleet interacting with trip requests. The fleet size is estimated based on waiting time, break-even price, and the number of rejected requests, assuming that the charging stations are pre-positioned and charging spaces are always available.

The contributions mentioned above tend to look at the problem more from an operational perspective rather than a strategic/planning one. They mostly focus on the detailed optimization of vehicle routing and charging, tracking each vehicle's activities independently and taking charging infrastructure either as given or considering it through post-processing or sensitivity analyses. The abovementioned optimization approaches most notably neglect the interactions between the number and location of charging facilities and the fleet size, as well as their joint impact on the overall system performance. While the models could theoretically be extended to consider these key design decisions and interactions of SAEV systems endogenously, severe tractability issues prevent them to be directly scaled to real-world large-scale settings. From an optimization perspective, tracking the flow and energy of individual vehicles in a system with hundreds of cars poses severe computational challenges, due to a significant increase in the number of variables and constraints. On the other hand, simulation has a hard time designing the optimal system, due to the computational burden of testing several different scenarios and viable combinations of input parameters.

This discussion underlines the need for integrated methods that allow modeling the problem at the required scale to make optimal decisions on key SAEV system design features, while capturing the interactions between charging infrastructure, fleet size, and vehicle operations. An interesting avenue in this respect is represented by the so-called flow-based optimization models. The flow-based optimization approach, with a space–time network, has been used to partially assess SAV systems (Liang et al., 2016; Tsao et al., 2018; Iglesias et al., 2018). It relies on the aggregation of vehicle movements into flows, which reduces the number of decision variables (when compared to vehicle routing). The application of the flow-based method in regional settings takes advantage of the low detail required and the low impact of congestion (considering the roads used and the distances involved). It has been shown that this approach can be applied to the design of regional real-sized SAV systems that serve interurban trips (Santos and Correia, 2021) not considering traffic congestion which is realistic in such a setting. Nevertheless, the use of the two-dimensional approach presented by Santos and Correia (2021) is unable to trace the energy consumed when vehicles are moving, and the energy charged when vehicles are plugged in, which hinders proper planning of a regional shared automated system that uses electric vehicles. To overcome this strong limitation in the context of electric mobility, the space–time network of this previous approach has been upgraded by adding a third dimension that tracks the energy level of the vehicles. This in turn allows extending the existing flow-based optimization frameworks to additionally design the location of charging facilities and model charging operations. The space–time-energy network concept was first introduced by Zhang et al. (2019). The model developed by the authors was designed for traditional (non-automated) one-way electric carsharing systems, mainly to optimize the charging movements. The authors assumed the existence of a given number of vehicles in the fleet, a fixed number of charging outlets per station, and identical charging power for each outlet with a constant charging rate. Relocations were not the focus due to the complexities of applying them to a carsharing system, but a simple analysis was conducted under a simplified assumption that relocation movements may occur only between certain stations and for pre-selected periods. In this paper, we push further the application of the three-dimensional network flow model to SAEVs using it to strategically design all its components in a regional context.

The flow-based integer programming (IP) optimization model that we propose is meant to support the early-stage design of a regional SAEV system, by optimizing the fleet (size and composition) and the charging facilities (number and location), considering a representative pattern of vehicle operations on a typical workday. Adding the energy dimension to the space–time network permits the accurate modeling of the energy of the vehicles in discrete states, which in turn enables to flexibly represent the movements of the vehicles with users, vehicle relocations, and charging operations alike. Furthermore, this modeling framework realistically accommodates charging stations with different charging rates and possibly nonlinear charging patterns, and it also allows studying heterogeneous fleets. Using a real-world case study, we implement our model to the design of a regional intercity SAEV system considering different scenarios through which we assess the influence of vehicle range and different seat layouts. To the best of our knowledge, this is the first time that a space–time-energy network flow-based optimization approach is applied to the strategic design of a SAEV system.

The paper is organized as follows. Section 2 presents the developed integer programming model. Section 3 describes the case study used in this research for testing the model, the region of Coimbra in Portugal. Section 4 includes the main results of running the model under different scenarios. The paper ends with the main conclusions, in Section 5.

2. Space-time-energy flow-based IP model

This section presents the formulation of the space–time-energy flow-based IP model to design a SAEV system in a regional context. The model is based on profit maximization and optimizes the vehicle movements (including relocations), the fleet, the location of charging facilities, and the energy flows related to vehicle charging.

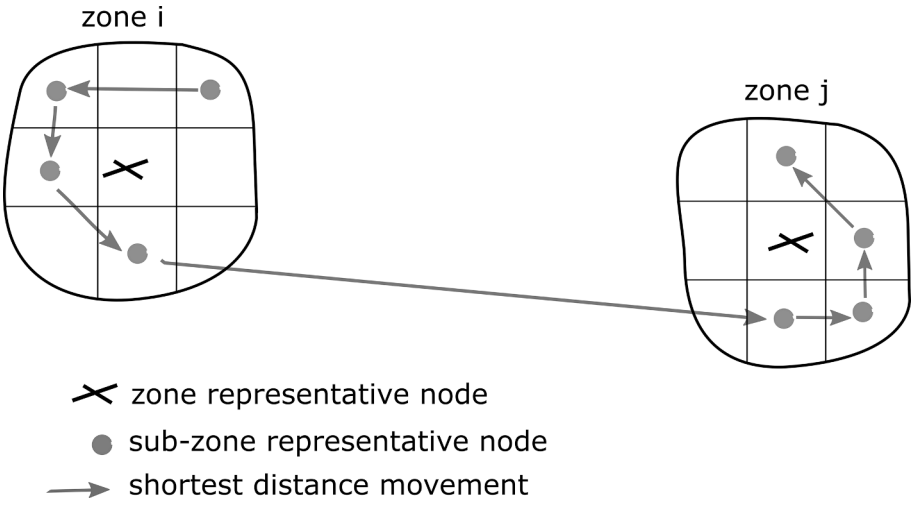

Fig. 1. Example of a single iteration of the Monte Carlo procedure used to estimate travel times.

2.1. Modeling assumptions

Before introducing our model notation, we present a set of assumptions upon which the model is built.

Planning perspective. It is assumed the existence of a SAEV system with BEVs controlled by a central operator that supplies inter-urban trips in a certain region. The model is aimed at providing decision support at the early planning stage of a SAEV system. In this sense, the focus is mainly on the design of the charging facilities and the sizing of the vehicle fleet, rather than vehicle routing and day of operations. By replicating flows in aggregate terms, the proposed model enables better strategic decisions and fosters compatibility with subsequent planning phases. The model is applied to a typical workday, assuming repeatability.

Model granularity. Similar to Santos and Correia (2021), we focus on the modeling of interurban trips, namely, trips between cities, or municipalities. In our network, physical nodes represent urban agglomerates, being spatially located in their focal centroid. Consistent with the level of aggregation, the model does not consider intra-urban and last-mile trips in detail but treats them in aggregate terms. This is attained by pooling demand at the city-pair level and developing an ad-hoc Monte-Carlo procedure to estimate an approximate travel time that incorporates the average intrazonal detours to pick-up (at the origin city) and deliver users (at the destination city). The procedure to estimate travel times is illustrated in Fig. 1 and detailed in Appendix A. We first divide each city into a set of smaller intrazonal areas, where each intrazonal area is represented by a node. The estimation of city-pair travel times is then conducted by simulating several vehicle movements for each origin–destination pair and then averaging their shortest path values. For each vehicle movement, the pick-up and delivery intrazonal nodes are randomly located. The number of pick-up and delivery nodes for each movement is equal in number to the vehicle capacity, and its spatial location is determined as a function of grid-based population estimates at a high resolution.

Demand. We assume that average daily demand estimates are available for every origin–destination pair and time period, and assume that all the trip requests are served by the SAEV system. Doing so, we do not model mode choice explicitly, nor consider any form of demand management (e.g., pricing policies or the possibility to anticipate or postpone trips). Instead, we focus on assessing an extreme scenario where the SAEV system design parameters are determined for providing all requested interurban trips in the region, while considering realistic input and scenarios that would make such a high rate of substitution realistic (e.g., traveling alone for a price lower than the current cost of using a private car, see Section 3 for details). Recent contributions have focused on developing effective methods to incorporate mode choice models into supply-side optimization models (Dong et al., 2016; Birolini et al., 2021; Pacheco Paneque et al., 2021). Most of these approaches could be implemented in our framework. However, this would require ad-hoc data to estimate a suitable mode choice model for the considered application, moreover the explicit consideration of demand–supply interaction in our space–time-energy network would likely add computational complexity that we wish to deal with in future research.

Service design. We let users share the same ride but restrict to rides that have in common both origin and destination zones, meaning that each vehicle travels directly from one zone to the other without picking up another user along the way. In fact, it has been demonstrated that multi-hop ride-sharing (Drews and Luxen, 2013) — despite being characterized by a great (theoretical) potential to reduce costs and making better use of vehicle capacities — is a poorly attractive travel option for users, who not only find themselves sharing the vehicle with strangers but also face higher waiting and travel times at the detriment of service level. Note that the focus on direct trips is even more reasonable in the interurban case, where even small detours would likely cause a significant increase in the overall travel times (especially in areas with spread population and lower road accessibility).

Charging. We assume that vehicles can charge when parked at a given charging facility (plug-in charging). Different charger types with different charging power can be used to charge vehicles. While using a certain charger type, the charging speed changes with the battery state of charge. The cost of charging is in accordance with the different electricity tariffs throughout the day.

Fleet. We formulate the problem assuming that the fleet is comprised by several types of vehicles, being each type characterized by

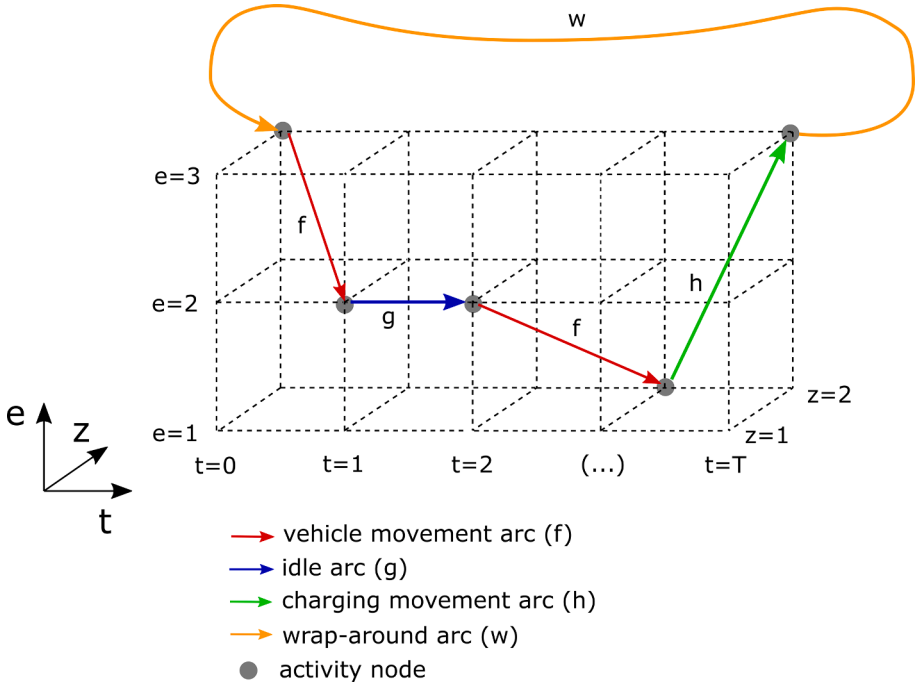

Fig. 2. Representation of the different activity arcs in a simplified network.

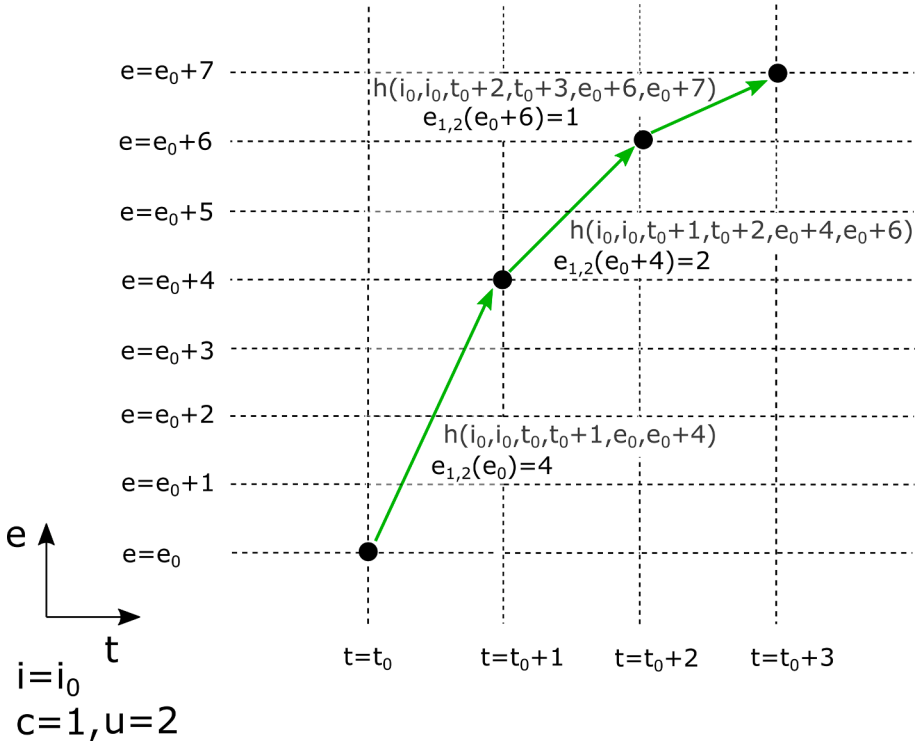

Fig. 3. Detailed example of the variation of the charging arcs with the SOC for a particular type of charger and vehicle type.

the number of seats, battery capacity, and energy consumption rate.

2.2. Mathematical formulation

Based on the previous assumptions, a flow-based integer programming model is built upon a three-dimensional space–time-energy network (see Fig. 2). This network is defined by a set of time instants $T = \{0, \cdots, t, \cdots, T\}$, a set of spatial nodes representing the zones $Z = \{1, \cdots, i, j, \cdots, Z\}$, and a set of energy levels $E = \{1, \cdots, e, \cdots, E\}$ that define its vertices. Note that the timestep size needs to be set according to the discretization of the energy levels, and vice versa. A set of charger types $C = \{1, \cdots, c, \cdots, C\}$ is defined to consider different charging powers. Additionally, a set of vehicle types $U = \{1, \cdots, u, \cdots, U\}$ is introduced to allow the simultaneous consideration of vehicles with different characteristics (e.g.: battery capacity, moving speed, speed of charging). The value E needs to accommodate all the energy level values for the types of vehicles $u \in U$ considered, that is $E = max_{u \in U}(E_u)$, being E_u the total number of energy levels of vehicle type u.

The network edges define the vehicle flows across the space–time-energy network. Each edge links two vertices, say (i, t_1, e_1) and (j, t_2, e_2), and therefore is uniquely identified by the six-element tuple $(i, j, t_1, t_2, e_1, e_2)$, where i and j are the origin and destination, respectively, t_1 and t_2 are the start and arrival times, respectively, and e_1 and e_2 represent the start and end energy levels. Not all edges describe feasible vehicle flows across the network. For instance, vehicles can only move ahead in time (i.e., it can never be that $t_2 \leq t_1$). Or, since vehicle movements consume energy and we do not allow for charging while traveling, the energy level can only decrease when vehicles move in space (i.e., it can never be that $e_2 \geq e_1$ when $i \neq j$). We denote the set of feasible edges as activity arcs (A). The two main activities considered are the movement of vehicles (with users and relocating) and the charging of vehicles. Moreover, we consider idle arcs to represent vehicles stationed (without charging) at a given node for a given period of time, and wrap-around arcs to ensure repeatability and flow conservation on a daily basis (Sherali et al., 2006), avoiding vehicle energy consumption with daily repetition. A visual representation is provided in Fig. 2. The set of A is thus subdivided in the following four subsets:

1) F that includes the **vehicle movement arcs** for serving users and for relocating. In this case, vehicles move in space, time and energy. Each moving arc is represented by $f = (i, j, t_1, t_2, e_1, e_2)$, where $i \neq j$, $t_2 > t_1$ and $e_2 < e_1$. The arrival time instant is defined as $t_2 = t_1 + t_{ij_u}$, being t_{ij_u} the time (in timesteps) needed to move from i to j by vehicle type u, estimated based on the procedure outlined in Appendix A. Similarly, the terminating energy level is equal to $e_2 = e_1 - e_{ij_u}$, being e_{ij_u} the energy (in energy units) needed to travel from i to j by vehicle type u.
2) H that includes the **charging arcs**. In this case, vehicles do not move in space but undergo a charging process that requires time to increase their energy level. Each charging arc is represented by $h = (i, i, t_1, t_2, e_1, e_2)$, with $i = j$, $t_2 = t_1 + 1$ and $e_2 > e_1$. The energy level at timestep t_2 is $e_2 = e_1 + e_{c,u}(e_1)$, being $e_{c,u}(e_1)$ the energy, in energy units, that is charged in one timestep using the charger type c to charge a vehicle of type u, starting from energy level e_1. Note that the value of $e_{c,u}(e_1)$ can vary with the battery state of charge (SOC). Fig. 3 has a detailed example of charging arcs.
3) G containing **idle arcs**. In this case, vehicles do not move either in space and energy, but only ahead in time. Each idle arc is thus represented by $g = (i, i, t_1, t_2, e_1, e_1)$, where $i = j$, $t_2 = t_1 + 1$ and $e_2 = e_1$.
4) W containing **wrap-around arcs**. Each arc is represented by $w = (i, i, t_1, t_2, e_1, e_2)$, and link the last timestep of the day to the first one. Wrapped around arcs do not represent any physical process but are modeling constructs to ensure repeatability and continuity in the network. Vehicles do not move in space and maintain the same energy level when transitioning to the next day, being $i = j$, $t_1 = T$, $t_2 = 0$, and $e_2 = e_1$.

Among the complete set of vertices, we define the set of activity-nodes, $N = \{1, \cdots, n, \cdots, N\}$, which include the subset of vertices that represent either the start or the end vertex of an activity arc. As clarified in Section 2.3, this allows reducing the mathematical size of the problem by filtering out vertices that will never be covered. The set of demand markets $M = \{1, \cdots, m, \cdots, M\}$ is also defined, which contains unique combinations of origin, destination, and time. Each demand market $m \in M$ is represented by a distinct tuple (i, j, t) that is used to index the demand parameters (trip requests from i to j at time t).

We now provide additional notation and formulate the flow-based IP model mathematically.

Additional sets:

F_u is the subset of movement arcs of vehicle type u, indexed by f;

$F_{m,u}$ is the subset of movement arcs of vehicle type u that serve the demand market m, indexed by f;

$F^{in}_{n,u}$ is the subset of inbound movement arcs of vehicle type u to activity node n, indexed by f;

$F^{out}_{n,u}$ is the subset of outbound movement arcs of vehicle type u from activity node n, indexed by f;

G_u is the subset of idle arcs of vehicle type u, indexed by g;

$G^{in}_{n,u}$ is the subset of inbound idle arcs of vehicle type u to activity node n, indexed by g;

$G^{out}_{n,u}$ is the subset of outbound idle arcs of vehicle type u from activity node n, indexed by g;

H_u is the subset of charging arcs of vehicle type u, indexed by h, for all charger types;

$H^{in}_{n,u}$ is the subset of inbound charging arcs of vehicle type u to activity node n, indexed by h for all charger types;

$H^{out}_{n,u}$ is the subset of outbound charging arcs of vehicle type u from activity node n, indexed by h for all charger types;

$H^{out}_{n,c}$ is the subset of outbound charging arcs from activity node n by charger type c, indexed by h for all vehicle types;

W_u is the subset of wrap-around arcs involving vehicle type u, indexed by w;

$W^{in}_{n,u}$ is the subset of inbound wrap-around arcs of vehicle type u to activity node n, indexed by w;

$W^{out}_{n,u}$ is the subset of outbound wrap-around arcs of vehicle type u from activity node n, indexed by w.

Parameters:

D_m is the demand, in number of users, for demand market $m \in M$ (i.e., number of trips requested from origin i, to destination zone j, and start time t);

p_m is the price to transport one user of demand market $m \in M$ (service price);

k_u is the vehicle capacity in number of seats of vehicle type u;

c_u is the daily fixed cost per vehicle of type u (includes depreciation, maintenance, and cleaning);

c_h is the cost for charging one vehicle using arc h. Recall that each charging arc is uniquely identified by the associated increase in energy levels and time of charging. Therefore, the cost associated with charging arcs can vary along the day according to the electricity tariffs charged by the provider;

c_f is the cost for moving one vehicle using arc f, excluding the energy cost already accounted for by c_h (e.g., it can include toll or congestion fees);

$c_{i,c}$ is the daily cost of locating a type c charging unit at zone i (value based on the installation and maintenance costs).

Decision Variables:

x_f is the number of vehicles moving (with users or relocating) using arc f;

y_h is the number of vehicles charging using arc h, considering all charger types;

s_g is the number of vehicles idle without being connected to the electric grid, using arc g;

z_w is the number of vehicles using wrap-around arc w;

$q_{i,c}$ is the number of charging stations of type c at zone i;

v_u is the total number of vehicles of type u in the system.

The model is formulated as follows:

$$\max(\pi) = \sum_{m \in M} p_m \times D_m - \sum_{h \in H} c_h \times y_h - \sum_{f \in F} c_f \times x_f - \sum_{c \in C} \sum_{i \in Z} c_{i,c} \times q_{i,c} - \sum_{u \in U} c_u \times v_u \tag{1}$$

Subject to:

$$\sum_{f \in F^{in}_{n,u}} x_f + \sum_{h \in H^{in}_{n,u}} y_h + \sum_{g \in G^{in}_{n,u}} s_g + \sum_{w \in W^{in}_{n,u}} z_w - \sum_{f \in F^{out}_{n,u}} x_f - \sum_{h \in H^{out}_{n,u}} y_h - \sum_{g \in G^{out}_{n,u}} s_g - \sum_{w \in W^{out}_{n,u}} z_w = 0, \ \forall n \in N, \forall u \in U \tag{2}$$

$$\sum_{w \in W_u} z_w = v_u, \ \forall u \in U \tag{3}$$

$$D_m \leq \sum_{u \in U} \left(k_u \sum_{f \in F_{m,u}} x_f \right), \forall m \in M \tag{4}$$

$$\sum_{h \in H^{out}_{n,c}} y_h \leq q_{i,c} \ \forall i \in Z, \forall n \in N, \ \forall c \in C \tag{5}$$

$$x_f \in \mathbb{N} \cup \{0\}, \forall f \in F \tag{6}$$

$$y_h \in \mathbb{N} \cup \{0\}, \forall h \in H \tag{7}$$

$$s_g \in \mathbb{N} \cup \{0\}, \forall g \in G \tag{8}$$

$$z_w \in \mathbb{N} \cup \{0\}, \forall w \in W \tag{9}$$

$$v_u \in \mathbb{N} \cup \{0\}, \forall u \in U \tag{10}$$

$$q_{i,c} \in \mathbb{N} \cup \{0\}, \forall i \in Z, \forall c \in C \tag{11}$$

The objective function (1) maximizes the total daily profit as a function of revenues and costs. The revenues result from charging a price to users for using the SAEV system, while the costs come from the energy consumed while charging, other expenditures associated with vehicle movements (e.g.: infrastructure fees), and system fixed expenses. The fixed expenses are related to the number of vehicles and charging facilities in the system. Constraint (2) ensures the conservation of flows in each activity node $n \in N$ for each vehicle type $u \in U$. In other words, for each vehicle type, the total outbound flow must be equal to the total inbound flow—as the sum of the number of vehicles allocated to any arc type— at every activity node. Constraint (3) sets the number of vehicles of each type $u \in U$ in the network, which is calculated using the wrap-around arcs. Constraint (4) links demand requests with vehicle movements and guarantees that the number of transported users does not surpass the aggregated vehicle capacity, such that the available capacity to serve a certain demand market $m \in M$ will at most accommodate the maximum number of passengers (i.e., equal to the seating capacity). Therefore, the procedure explained in Appendix A, which simulates as many requests as there is vehicle capacity at each

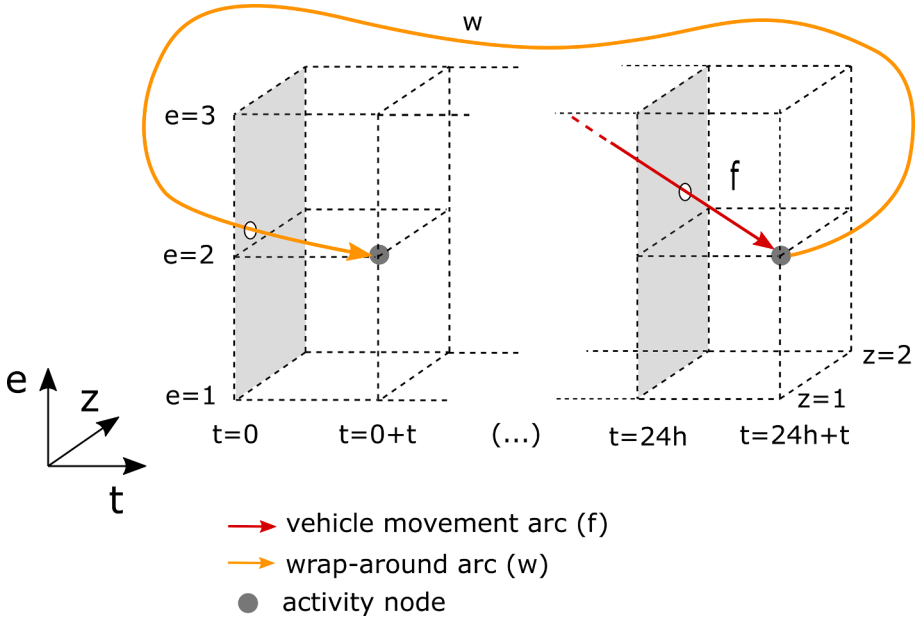

Fig. 4. Representation of a compound wrap-around arc.

iteration, ensures that the travel time is enough, on the conservative side, for any possible number of passengers traveling inside the vehicle, for the considered vehicle type. Constraint (5) limits the number of vehicles charging simultaneously at each zone to the number of installed charging stations. Expressions (6) to (11) define the domain of the variables.

There are some special considerations when building the abovementioned space–time-energy network, namely concerning to first and last timestep overlap, and wrap-around arcs.

First and last timestep overlap – A way of using wrap-around arcs is to overlap the first and last timesteps, though we need to assure that the correspondent demand requests are accounted for only once. The demand is defined for an entire day, being the first requests for the instant zero coincident to the time instance corresponding to 24-hour. In this work, we consider that the 24-hour time instance does not have any request, since these were already accounted for in the time instance zero.

Wrap-around arcs – To guarantee the continuity of the network, two types of wrap-around arcs are considered: simple wrap-around arcs, and compound wrap-around arcs. The simple wrap-around arcs connect idle vehicles from the 24-hour instant back to zero time instant (see Fig. 2), and work together with the activity arcs that terminate within the unitary time duration (e.g., idle and charging arcs). However, some trips may be requested in late evening (e.g. 11.30 pm), such that their corresponding moving arc would surpass the 24-hour threshold. In this case, the corresponding moving arc is added to the network and allowed to overpass the 24-hour limit, terminating at time instant $24+t$. Additionally, a compound wrap-around arc is added to connect directly this terminating node at time $24+t$ to the correspondent node of the next day at time t (see Fig. 4). In consequence, the time duration of the modeled network, T, increases in the number of necessary timesteps beyond the 24-hour period to accommodate the new activity nodes. The use of the compound wrap-around arcs in conjunction with the activity arcs that extend beyond the 24-hour instance allows accounting for the contribution of the vehicle movement arc in the objective function without compromising the constraints, particularly for constraint (3), which computes the fleet size as the sum of z_w across wrapped around arcs. Theoretically, we could replace the surpassing arc and related compound wrapped around arc with a "backward moving arc". However, this would undermine the validity of flow balance and fleet size constraints.

2.3. Problem size and arc generation

The mathematical model (1) to (11) has six sets of decision variables (x_f, y_h, s_g, z_w, $q_{i,c}$, and v_u). The number of decision variables in set x_f is equal to the number of arcs $f \in F$, which, assuming a fully connected network, totalize $(Z^2 - Z) \times (T^2 - T)/2 \times \sum_{u \in U}\left({E_u}^2 - E_u\right)/2$. The subtraction of Z from Z^2 is because the model does not consider movements inside the same zone. The multiplication term $(T^2 - T)/2$, which results from the subtraction of $\sum_{t=0}^{T} t$ from T^2, is a consequence of not having movements from time t_2 to t_1, being $t_2 > t_1$. Similarly, the multiplication term $({E_u}^2 - E_u)/2$, obtained from the subtraction of $\sum_{e=1}^{E_u} e$ from ${E_u}^2$, is a consequence of the energy decreasing while vehicles move. The sum of $u \in U$ is there to accommodate the distinct total number of energy levels for each of the vehicle types considered. For the set y_h the total number of decision variables is equal to $Z \times C \times (T^2 - T)/2 \times \sum_{u \in U}({E_u}^2 - E_u)/2$. Since any zone is a possible location to charge vehicles with any type of charger the multiplication $Z \times C$ must be added. The term $(T^2 - T)/2$ has the same meaning as previously described for the set x_f. The term $({E_u}^2 - E_u)/2$ is due to energy

Table 1
Number of decision variables per set.

Decision variable sets	Number of variables
x_f	$(Z^2 - Z) \times (T^2 - T)/2 \times \sum_{u \in U}(E_u{}^2 - E_u)/2$
y_h	$Z \times C \times (T^2 - T)/2 \times \sum_{u \in U}(E_u{}^2 - E_u)/2$
s_g	$Z \times (T-1) \times \sum_{u \in U} E_u$
z_w	$Z \times \sum_{u \in U} E_u$
$q_{i,c}$	$Z \times C$
v_u	U

increasing while vehicles charge. The sum of $u \in U$ is, once again, to include the arcs for each vehicle type. The number of decision variables related to s_g is equal to $Z \times (T-1) \times \sum_{u \in U} E_u$. For the set z_w the total number of variables is equal to $Z \times \sum_{u \in U} E_u$ which is the total number of simple wrap-around arcs (if compound wrap-around arcs are used, an additional variable for each compound arc should be added to the cardinality of the set z_w). The set $q_{i,c}$ is of size $Z \times C$, meaning that each zone can receive chargers of any type. Finally, the size of the set v_u is equal to the number of vehicle types considered, which is U. Table 1 summarizes what was previously described. This process is a simple way to assess the number of variables considering all degrees of freedom of the model.

To reduce the size of the problem, we pre-process the input data to only consider the necessary arcs and nodes (see Algorithm 1). This reduces the number of decision variables, namely the ones related to x_f and y_h, which depend directly on the number of arcs. The model parameters are used to create all the possible arcs, for each vehicle type, considering the characteristics of the application scenarios, namely demand and travel time. The resulting activity node set, valid for all vehicle types, contains all the nodes obtained by varying $i = 1 \cdots Z, t = 0 \cdots T$, and $e = 1 \cdots E$ (being E the maximum number of energy levels needed to accommodate all vehicle types $u \in U$ considered), due to the unitary size in the time dimension of idle and charging arcs. Although, since activities described by arcs $f \in F$ extend for longer periods and continue for the next day ($t > T$), some additional nodes have to be created to support these and the compound wrap-around arcs. The compound wrap-around arcs complemented by the simple wrap-around arcs (created when defining the idle arcs) complete the needed connections between the current day and the next day. The charging arcs incorporate the variation of charging speed with the battery SOC for each type of charger station.

Algorithm 1: define the necessary arcs and nodes

1: Set the timestep size
2: Discretize energy levels according to timesteps (size of energy level = energy needed to travel during one timestep)
3: Insert demand values D_m for each market $m(i,j,t)$
4: Insert travel time values t_{ij_u} (in timestep units – Appendix A); as well as the energy e_{ij_u} (in energy level units)
5: Create all the nodes for the space–time-energy network ($i = 1 \cdots Z, t = 0 \cdots T, e = 1 \cdots E$). The value E needs to accommodate the energy level values for the types of vehicles $u \in U$ considered ($E_u = \{1, \cdots, e, \cdots, E_u\}$).
For each $u \in U$
6: Vehicle movement arcs with users:
  For each $m(i,j,t) \in M$
    For each $e \in E_u \wedge e - e_{ij_u} \geq 1$
      Create arc $f \in F_u$ with $i_1 = i$, $i_2 = j$, $t_1 = t$, $t_2 = t + t_{ij_u}$, $e_1 = e$, $e_2 = e - e_{ij_u}$
      Identify arc f as belonging to the subset $F_{m,u}$
    End For
  End For
7: Other vehicle movement arcs (associated to relocations):
  For each $i \in Z, j \in Z, t \in T \wedge i \neq j \wedge t < T$
    For each $e \in E_u \wedge e - e_{ij_u} \geq 1$
      Create arc $f \in F_u$ with $i_1 = i$, $i_2 = j$, $t_1 = t$, $t_2 = t + t_{ij_u}$, $e_1 = e$, $e_2 = e - e_{ij_u}$
    End For
  End For
8: Additional nodes and corresponding compound wrap-around arcs:
  For each arc $f(i_1, i_2, t_1, t_2, e_1, e_2) \in F_u$ with $t_2 > T$
    Create the additional node i, t,e with $(i = i_2, t = t_2, e = e_2)$
    Create the compound wrap-around arc $w(i_1^{'}, i_2^{'}, t_1^{'}, t_2^{'}, e_1^{'}, e_2^{'}) \in W_u$
      with $i_1^{'} = i_2^{'} = i_2$, $t_1^{'} = t_2$, $e_1^{'} = e_2^{'} = e_2$
      $t_2^{'} = t_2 - T$
  End For
9: Idle arcs and corresponding simple wrap-around arcs:
  For each $i \in Z, t \in T, e \in E_u \wedge t \leq T$
    If $t < T$ then
      Create arc $g(i_1, i_2, t_1, t_2, e_1, e_2) \in G_u$ with $i_1 = i_2 = i$, $t_1 = t$, $t_2 = t + 1$, $e_1 = e_2 = e$
    Else
      Create arc w $(i_1, i_2, t_1, t_2, e_1, e_2) \in W_u$ with $i_1 = i_2 = i$, $t_1 = T$, $t_2 = 0$, $e_1 = e_2 = e$
    End If
  End For
10: Charging arcs:
  For each $c \in C, e \in E_u \wedge e < E_u - 1$

(continued on next page)

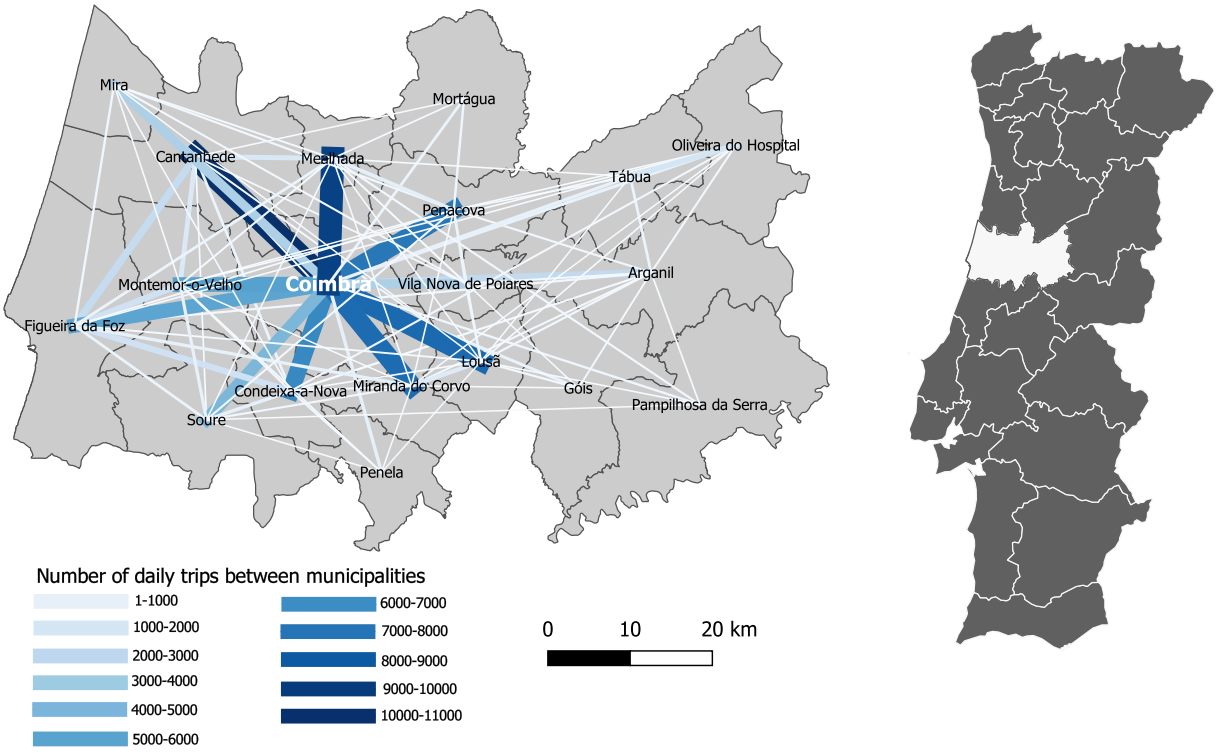

Fig. 5. Representation of the daily trips between the Coimbra region municipalities (based on results from TIS.pt, 2009).

(*continued*)

Algorithm 1: define the necessary arcs and nodes

Insert $e_{c,u}(e) = \#$ of energy levels charged in one timestep by a charger type c connected to a vehicle type u, starting at e
End For
For each $c \in C$, $i \in Z$, $t \in T, e \in E_u \wedge t < T$
If $e + e_{c,u}(e) \leq E_u$ then
Create arc $h(i_1, i_2, t_1, t_2, e_1, e_2) \in H_u$
with $i_1 = i_2 = i$, $t_1 = t$, $t_2 = t + 1$, $e_1 = e, e_2 = e + e_{c,u}(e)$
End If
End For
11: Remove duplicates from the sets of arcs F_u, G_u, H_u, W_u
End For
12: Remove duplicates from the set of nodes

3. Case study

The space–time-energy flow-based IP model was used to assess the influence of vehicle range in the optimal configuration (profitwise) of SAEV systems, which includes fleet size, charging facilities, and vehicle operations. For that, different vehicle types were considered for the car fleet. The adopted case study is the Coimbra region, a level-3 NUTS region of the Portuguese territory with 19 municipalities, represented in Fig. 5 (the NUTS is a hierarchical division system of the European Union economic territory). This region has an area of 4,335 square kilometers and is populated by 460 thousand inhabitants (INE, 2011). The occupation of the territory is polycentric with significant distances between the smaller cities, being the Coimbra municipality (the one that names the region) the most important one. As it can be seen in Fig. 5, most OD pairs of the region do not have enough demand to justify large investments in public transport projects for interurban trips, leading to high car dependency. The implementation of a SAEV system in the region would improve the accessibility to higher quality transport services, namely in the less dense areas where public transport is characterized by having a low frequency and longer routes. This study considers the introduction of a SAEV system to serve all the intermunicipal trips with both ends inside the region. The inner municipal trips are assumed to be well served by local public transport.

The region of Coimbra is divided into different municipalities, each one is a zone in the model from which trips depart and arrive. For computing an approximated pick-up and drop-off time inside each zone (municipality), as explained in Appendix A, we adopted the smallest administrative units (parishes) as subzones. Centroids were used as the representative spatial nodes of both territorial entities. The average distance between zone centroids is 53 km, being the shortest equal to 12 km, and the longest equal to 137 km. The demand data was retrieved from the Mondego mobility survey (TIS.pt, 2009), which is still the most complete one available for the

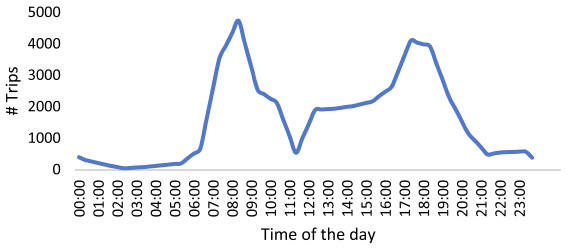

Fig. 6. Hourly distribution of the daily trips between the Coimbra region municipalities.

Table 2
Characteristics of the considered vehicle types.

Vehicle type	Short-range	Medium-range	Long-range
Passenger capacity (seats)	1 and 4	1 and 4	1 and 4
Battery capacity (kWh)	40	60	80
Consumption (kWh/100 km)	17	17	17
Range (km)	235	352	470
Max AC charging (kW)	22	22	22
Max DC charging (kW)	100	100	100
Acquisition cost per unit (€)	30,000	45,000	60,000
Cost per vehicle (€/day)	20	30	40
Data inspired by:	Renault Zoe, Nissan Leaf.	Hyundai Kona, Kia e-Soul.	Tesla Model 3 long range

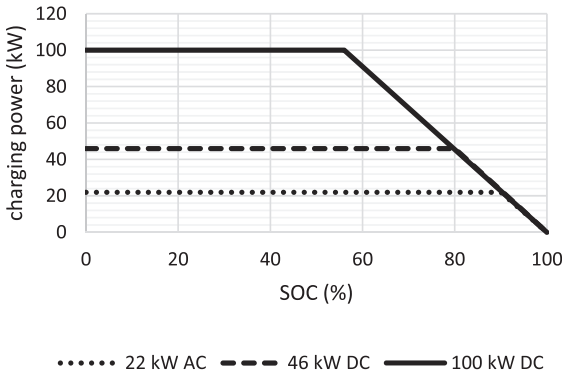

Fig. 7. Charging curves for the considered charging powers (based on data from Fastned, 2021).

region. According to this survey, the Coimbra region has about 116 thousand daily intermunicipal trips performed by motorized transport, representing an aggregated distance of 3.71 million kilometers. The demand D_m, was generated using a Poisson process with rates equal to the hourly intermunicipal motorized trip values for each OD pair, observed in the survey. The hourly distribution of the obtained trip demand is represented in Fig. 6. The travel times were calculated using the process described in Appendix A. The travel times between centroids, needed as input data for this process, were determined using Google Maps (Google, 2019). The obtained values were considered to be constant throughout the day since congestion is not a very significant issue concerning interurban trips in the case study region. Integrating travel time stochasticity is not that straightforward, but the model could be easily extended to accommodate different average travel times as a function of time of the day. The scope of analysis is a typical day of operation, being the 24-hour period subdivided into timesteps of 20 minutes.

The characteristics of BEV models currently available in the market (ev-database, 2021) served as a basis to define three vehicle types depending on their range: short-range, medium-range, and long-range (see Table 2). These vehicle types allow studying the variation of the design characteristics of SAV services with the type of vehicle used in the fleet. The number of energy levels considered for each vehicle type is 12, 18 and 24, respectively (it assumes that one energy level contains the necessary energy to travel during one timestep at the average travel speed verified in the region for the intermunicipal trips, which is 60 km/h). Note that all the vehicle types have enough battery capacity to travel the longest distance inside the region on a single charge. The price per day includes depreciation of 20% per year during the first three years (TheAA.com, 2019), as well as insurance, cleaning and maintenance costs. For each vehicle model, two different vehicle capacity layouts are used to differentiate two possible services that can potentially be provided in the region: a service that transports one passenger per vehicle, increasing the comfort inside the vehicle, and allowing an experience similar to a private vehicle; and, a service allowing pooling inside a vehicle with a layout that allows the transportation of a

Table 3
Costs of a single port unit for each charger type.

Charger type	22 kW AC	46 kW DC	100 kW DC
Acquisition cost (per unit)	2,700 USD (pedestal with low level data collection)	10,000 USD (low power DC fast charger)	30,000 USD (mid-price DC fast charger)
Installation cost (per unit)	2,000 USD (fleet setting)	8,500 USD (sites using existing electrical service)	8,500 USD (sites using existing electrical service)
Total (per unit)	4,700 USD = 3,905€	18,500 USD = 15,373€	38,500 USD = 31,993€
Daily total (per unit)* *3 years payment without interests	4 €/day	15 €/day	30 €/day

Table 4
Price of electric energy based on a tariff plan from a Portuguese provider.

Period	Time	Price of kWh (Euro)
Empty	21h-8h	0.09
Full	8h-9h and 11h–18h	0.15
Peak	9h-11h and 18h-21h	0.28

Table 5
Scenarios and its main characteristics.

Designation	Characteristics	Number of scenarios
SAEV-S	A fleet with short-range vehicles; Chargers owned by the company; Vehicle capacities tested: 1 and 4 seats.	2
SAEV-M	A fleet with medium-range vehicles; Chargers owned by the company; Vehicle capacities tested: 1 and 4 seats.	2
SAEV-L	A fleet with long-range vehicles; Chargers owned by the company; Vehicle capacities tested: 1 and 4 seats.	2
SAEV-All	A fleet designed considering the use of the three types of vehicles - short, medium and long-range; Chargers owned by the company; Vehicle capacities tested: 1 and 4 seats.	2

maximum of four passengers simultaneously. The one-seat layout has a seating capacity close to the average private vehicle occupancy rate for the region (1.4 passengers) and serves as a reference to what represents the system design and performance if the vehicle layout had a comfortable inner space with complete privacy for the passenger to perform other activities while travelling. Note that the case study region is characterized by having a Mediterranean climate (dry summers, and mild, wet winters), therefore the adopted vehicle consumption rates are based on "highway mild weather" values (ev-database, 2021). These values were chosen for being higher than the values presented for "combined mild weather" situations (ev-database, 2021) such as the one in the studied region. This allows to have a charging network that can accommodate the variability in terms of energy consumption.

The charging curves used for each vehicle type are based on the charging data for the same car models used as references (Fastned, 2021). To emulate what happens in reality, it is considered that the charging rate of batteries is stable for the initial charging levels, while it decreases afterwards at a steady rate with the state of charge (SOC) of the vehicle battery. This behavior depends on the considered charging power and is assumed to be the same for all vehicle types. The adopted charging curves are represented in Fig. 7. The increment of energy levels of each charging arc is determined based on the discretization of these curves.

Additionally, we assumed that the SAEV service provider pays for the installation and maintenance of the charging stations, as well as for the electric energy consumed. This case study considers 22 kW AC chargers, 46 kW DC chargers, and 100 kW DC chargers, which is similar to the charging technology currently available in the region. Due to the unavailability of related data, the cost for each charging port is based on Smith and Castellano (2015) and can be seen in Table 3. The total cost per day of using a single charger port considers that the equipment is paid in three years without interest, and includes the maintenance costs. For the electric energy costs, we use the tariffs charged by the Portuguese company edp (edp, 2021) for the tri-hourly daily cycle plan. This plan considers three time periods within a day, characterized by different kWh unitary prices. These time periods are dependent on the seasonal clock time in use (winter or summer). For this study, we established the electricity prices and cycle periods based on the values from the providers' winter time tariff plan (see Table 4).

The prices charged by the SAEV system operator to users were established based on the cost of using the private car in the region. The cost of using the private car for each pair of zones was obtained from a trip planning website (ViaMichelin, 2021) which includes petrol and tolls. The application of a linear regression to these values resulted in an average value of 0.15 Euro per kilometer with an R-squared value of 0.96. The price charged to each passenger for the service transporting one passenger per vehicle was assumed to be equal to 0.12 Euro per kilometer, which represents a 20% discount from the cost of using a private vehicle in the region. On the other hand, the price charged to each passenger for the service with pooling was considered to be equal to 0.06 Euro per kilometer, half of the price charged for the service with a single passenger. The prices are thus lower than the cost of using the private car to provide an advantage in using the system.

Eight different scenarios, corresponding to the same number of system configurations (see Table 5), were tested in this work. These

Table 6
Model setting characteristics and GAPs for the considered scenarios.

Scenario		#zones	#time steps	#energy levels	#nodes	#arcs	GAP in 10,000 s
SAEV-S	1-seat	19	72	12	17,162	339,120	0.04%
	4-seats	19	72	12	17,240	327,967	0.03%
SAEV-M	1-seat	19	72	18	25,832	543,372	0.20%
	4-seats	19	72	18	25,988	532,297	0.07%
SAEV-L	1-seat	19	72	24	34,502	747,624	0.17%
	4-seats	19	72	24	34,736	736,627	0.04%
SAEV-All	1-seat	19	72	24	34,502	1,630,116	0.01%
	4seats	19	72	24	34,736	1,596,891	0.07%
Sensitivity analysis (SAEV-S 4-seats):							
a) Equal charger cost		19	72	12	17,240	327,967	0.01%
b) Flat tariff plan		19	72	12	17,240	327,967	0.10%
c1) −10% demand		19	72	12	17,240	327,967	0.01%*
c2) +10% demand		19	72	12	17,240	327,967	0.78%*
c3) demand shift		19	72	12	17,240	327,967	0.37%*

* solved using the altered model formulation (12) to (14) with pre-determined values for some decision variables, as described in Section 4.4. For these scenarios the 10,000 seconds limit was turned off.

Table 7
Optimization results.

	1-seat layout				4-seats layout (with pooling)			
	SAEV-S	SAEV-M	SAEV-L	SAEV-All	SAEV-S	SAEV-M	SAEV-L	SAEV-All
Service price (€/km)	0.12	0.12	0.12	0.12	0.06	0.06	0.06	0.06
Revenue (€/day)	575,329	575,329	575,329	575,329	287,665	287,665	287,665	287,665
Total cost (€/day)	384,939	503,326	630,942	384,925	194,185	244,011	298,685	193,982
- fleet cost (€/day)	265,240	397,860	530,560	265,240	122,240	181,020	241,320	122,190
- energy cost (€/day)	106,672	89,438	83,310	106,666	63,534	55,646	47,925	63,459
- chargers cost (€/day)	13,027	16,028	17,072	13,019	8,411	7,345	9,440	8,333
Profit (€/day)	**190,390**	**72,003**	**−55,613**	**190,404**	**93,480**	**43,654**	**−11,020**	**93,683**
Ratio profit/revenue (%)	33%	13%	−10%	33%	32%	15%	−4%	33%
Fleet size	13,262	13,262	13,264	13,262	6,112	6,034	6,033	6,071
- # of S range vehicles	13,262	–	–	13,262	6,112	–	–	5,994
- # of M range vehicles	–	13,262	–	0	–	6,034	–	77
- # of L range vehicles	–	–	13,264	0	–	–	6,033	0
Total number of chargers	3,243	4,007	4,268	3,241	1,836	1,817	2,360	1,843
- # of 22 kW chargers	3,238	4,007	4,268	3,236	1,739	1,810	2,360	1,757
- # of 46 kW chargers	5	0	0	5	97	7	0	85
- # of 100 kW chargers	0	0	0	0	0	0	0	1
Total energy bought (kWh/day)	937,553	925,987	925,548	937,507	522,383	520,116	515,873	522,789
- energy moving users (kWh/day)	788,624	788,624	788,624	788,624	497,039	497,086	497,135	497,000
- relocation energy (kWh/day)	148,929	137,363	136,924	148,883	25,344	23,031	18,737	25,789
Energy bought per period:								
- empty period (%)	60.4	89	100	60.4	49.3	71.7	95.2	49.2
- full period (%)	39.6	11	0	39.6	49.8	28.3	4.8	50.0
- peak period (%)	0	0	0	0	0.9	0.0	0.0	0.8
Total trips served/day	116,050	116,050	116,050	116,050	116,050	116,050	116,050	116,050
Trips per vehicle/day	8.8	8.8	8.7	8.8	19.0	19.2	19.2	19.1
Avg. travel time/passenger (min)*	33	33	33	33	59	59	59	59
Total # of relocations/day	32,678	30,388	31,580	33,670	5,681	5,442	4,395	5,778
Vehicle time:								
- moving users (%)	25.0	25.0	25.0	25.0	34.2	34.7	34.7	34.4
- relocation time (%)	4.7	4.4	4.3	4.7	1.7	1.6	1.3	1.8
- idle time excluding charging (%)	54.7	55.2	56.0	54.7	47.0	45.0	45.3	46.5
- charging time (%)	15.6	15.4	14.7	15.6	17.1	18.7	18.7	17.3
Vehicles moving with users:								
- avg. time/veh.mov. (min)*	41	41	41	41	94	94	94	94
- avg. # of passengers/veh.mov. (veh.mov. = vehicle movement)	1	1	1	1	3.6	3.6	3.6	3.6

* Note that discrepancies among these two values are due to the discretization adopted in the paper.

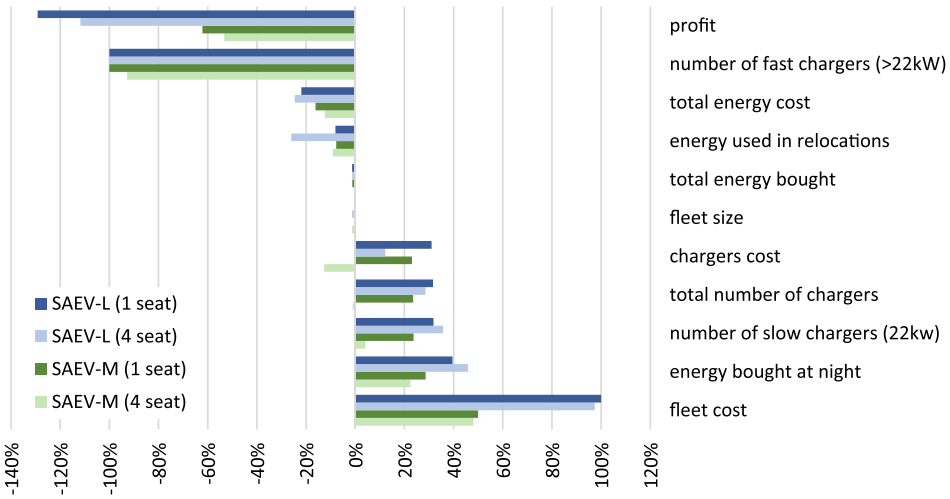

Fig. 8. Percentual differences relative to the SAEV-S scenario for both 1-seat and 4-seat vehicle layouts.

scenarios resulted from considering the two in-vehicle seat layouts (1 and 4 seats) for each of the three vehicle types (short, medium, and long-range), in addition to two scenarios with multiple vehicle fleets that include the three vehicle types, each one testing a different seating capacity (1 and 4 seats). All of them admit the possibility of having all three types of charger stations (22, 46, and 100 kW) installed and used to power the vehicles.

4. Results

This section presents the results obtained for the SAEV scenarios by applying the space–time-energy flow-based IP model. First, an assessment of the SAEV system design parameters using a fleet comprised of only one vehicle type is presented. This allowed analyzing the effect of vehicle range on profit (Section 4.1), vehicle operations, and charging network (Section 4.2). Then, a study of the optimal configuration of the SAEV system by using a combination of the three vehicle types is included (Section 4.3). Lastly, a sensitivity analysis is performed by introducing variations to some parameters (Section 4.4). The solver time limit was set for 10,000 seconds and all scenarios solved with the mathematical model (1) to (11) returned near optimal solutions with GAP values ranging from 0.01% to 0.20% (see Table 6). The software used was Xpress which ran in a desktop computer with an Intel Core i7-8700 processor with 3.20 GHz processing speed, a Solid-State Drive, and 16 GB of RAM. The described performance includes the scenarios SAEV-All, in which the higher number of arcs (between 2 and 3 times more arcs than the other scenarios) only affected the time to load the input file. In Appendix B we report a more detailed assessment of the convergence pattern.

As a side note, it should be mentioned that the base results in this work can differ from the ones in Santos and Correia (2021), even though they both focus on the same case study. This is due to the improvement in determining the travel times, specifically the use of real routes instead of straight lines for the intra-municipal movements (see Appendix A), and the explicit consideration of energy consumption and charging dynamics.

4.1. Profitable system configurations and aggregated effects of vehicle range variation

For a company, the best service configuration is the one that maximizes profits. Looking at the results in Table 7, it can be observed that the system for the scenarios including short-range vehicles (SAEV-S) return the highest profit. This is mainly related to the lower cost associated with buying a short-range vehicle fleet. The vehicles in the fleet represent the most important cost component and its weight directly affects the profit which decreases as the unitary cost of vehicles increases. In fact, profit and fleet costs are in the extremes of Fig. 8, where the percentual variations (increase and decrease) of the most relevant key performance indicators are presented. Compared to other vehicle ranges, we can observe that the optimized configurations with medium-range vehicles (SAEV-M) still achieve a profit, though the ones with long-range vehicles (SAEV-L) result in daily losses (see Table 7).

As a proxy to how efficiently a company turns sales into profits, the return on sales (computed as the ratio between profit and revenue) when deploying short-range vehicles is higher than 30%, for the conditions of the case study. The service with one passenger per vehicle gives a return on sales equal to 33%, while with pooling (4-seats vehicle layout) the result is a ratio of 32%. The values are similar due to the difference in the service price per kilometer charged to each user which is reduced by half for the service with pooling. The reported difference has a direct impact on the absolute profit value, which is approximately two times higher for the service using short-range vehicles with one passenger per vehicle (190,390€) when compared to the service with pooling (93,480€).

Observing closely the variation of the results with the vehicle range (see Table 7 and Fig. 8), we can identify other relevant aspects related to the optimal system configuration:

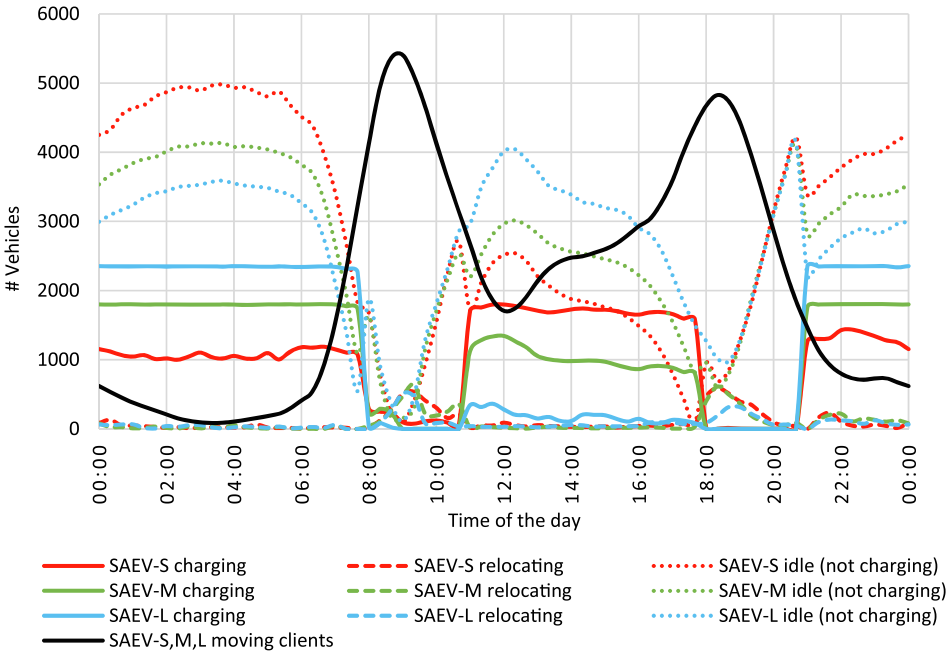

Fig. 9. State of the vehicles during the day for the scenarios where vehicles have 4-seats.

i. Increasing the battery capacity of the vehicles facilitates battery charging during the night period, when energy is cheaper and there is time to take advantage of cheaper slow chargers. As it can be seen in Table 7, the total number of chargers increases from 3243 to 4268 for the scenarios with 1-seat, and from 1836 to 2360 for the scenarios with 4-seats. The increment in the battery capacity allows vehicles to charge when the energy is cheaper. Therefore, the charging operations are concentrated in periods with lower tariffs, with more vehicles charging simultaneously. The savings in the energy cost compensate for the increment in the installation and maintenance costs of the additional chargers. Taking the SAEV-L service with 1-seat as an example, the increase in the cost of having more chargers than the SAEV-S scenario is equal to 4045 Euro per day, while the savings in energy reach an amount of 23,362 Euro per day. Note that the decrease in the number of chargers required between the SAEV-S and SAEV-M with pooling is an exception to the previous claim. This is due to the SAEV-S system needing more fast chargers (46 kW), essential to fill the batteries of short-range vehicles in the middle of the day (more information about this in Section 4.2), which increases the total number of chargers to a value rather higher than for the SAEV-M.

ii. The adoption of higher range vehicles reduces the energy spent in relocations and increases the energy charged during the night period, which is when the electricity is cheaper. As observed in Table 7, the energy spent on relocations decreases from 149 MWh to 137 MWh for the scenarios with 1-seat, and from 25 MWh to 19 MWh for the scenarios with 4-seats. On the other hand, the percentual of the total energy that was bought during the empty period (cheaper tariff) increases from 60% to 100% for the scenarios with 1-seat and from 49% to 95% for the scenarios with pooling.

iii. The importance of having fast chargers reduces with the increase of the vehicle battery capacity since vehicles do not need to charge so much during the day and can fulfil their needs when the idle period is longer and the energy is cheaper. This is more evident in the scenarios with 4-seats whereby the number of 46 kW chargers decreases from 97 (SAEV-S) to 0 (SAEV-L), and the energy bought during the day (full and peak periods) decreases from 51% to 5% (see Table 7). None of the optimal system configurations included 100 kW chargers, which is the fastest charger available for installation.

iv. Lower battery capacity can lead to more vehicles than the ones needed to serve the demand if the battery capacity were not a limitation, which is related to the possibility of having vehicles charging during the peak demand periods (when more users need to be served). This can be verified in Table 7 for the scenarios with pooling where the fleet size decreases from 6112 vehicles (SAEV-S) to 6033 vehicles (SAEV-L). The optimization process can also return a slightly higher number of vehicles as the range increases if the daily cost of having a few more vehicles is lower than all the other costs combined. This happens for the scenarios with 1-seat vehicles where the size of the fleet is stable at 13,262 vehicles for both the SAEV-S and SAEV-M system configurations, though it adds two more vehicles in the case of the SAEV-L configuration (see Table 7).

4.2. Detailed analysis of vehicle operations and charging network usage as vehicle range increases

The state of the vehicles and the usage of the charging infrastructure at each timestep were analyzed considering all system configurations. The scenarios using vehicles with an interior layout of 1-seat and the ones with 4-seats revealed similar behavior as the vehicle range increases. As a consequence, we opted to include in this description the analysis of the scenarios with vehicles with 4-

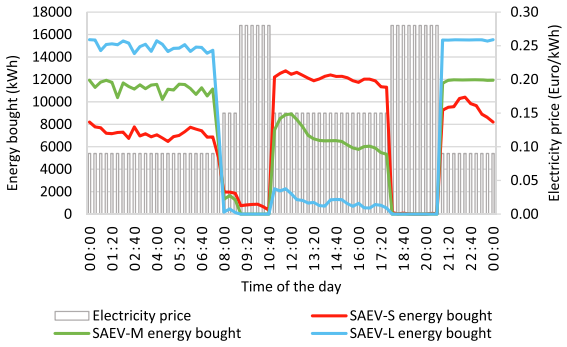

Fig. 10. Quantity of energy bought vs electricity price for the scenarios with 4-seats.

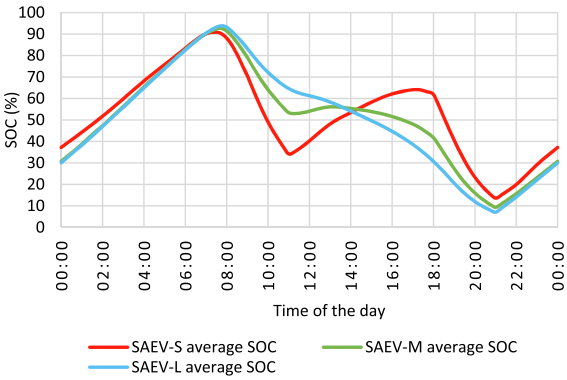

Fig. 11. Average battery state of charge (SOC) for the scenarios with 4-seats.

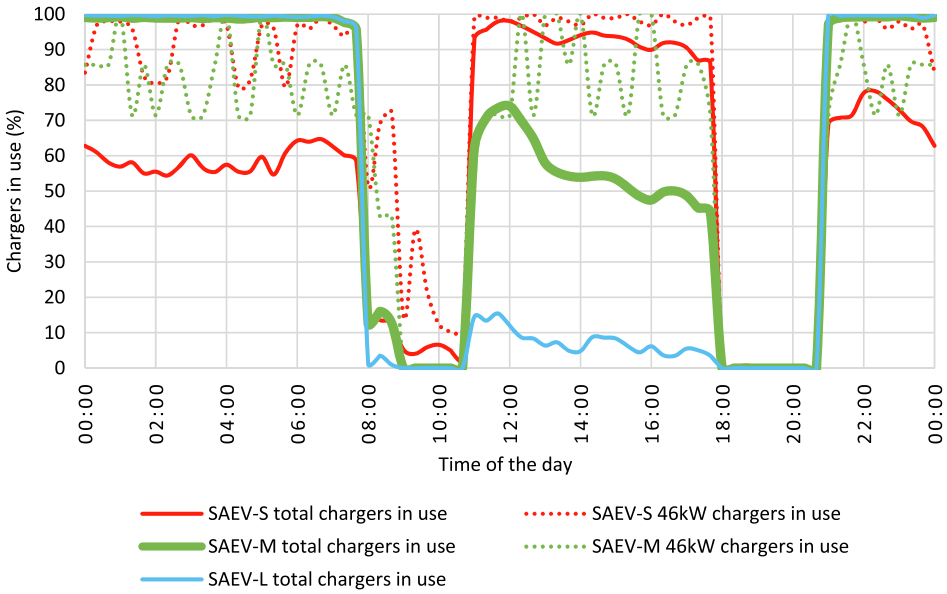

Fig. 12. Percentage of chargers in use (total and type 2) for the scenarios with vehicles with 4-seats.

seats, which represent a system where more trips are served per vehicle resulting in higher charging needs per vehicle.

The values for the decision variables of the IP model allowed to detail the optimized system operations along the day and to better understand what was revealed by the aggregated optimization results in Section 4.1. In Fig. 9, where the state of the vehicles along the day is presented, we can see that the need to charge during the day decreases with the range of the vehicle type used in the fleet. The

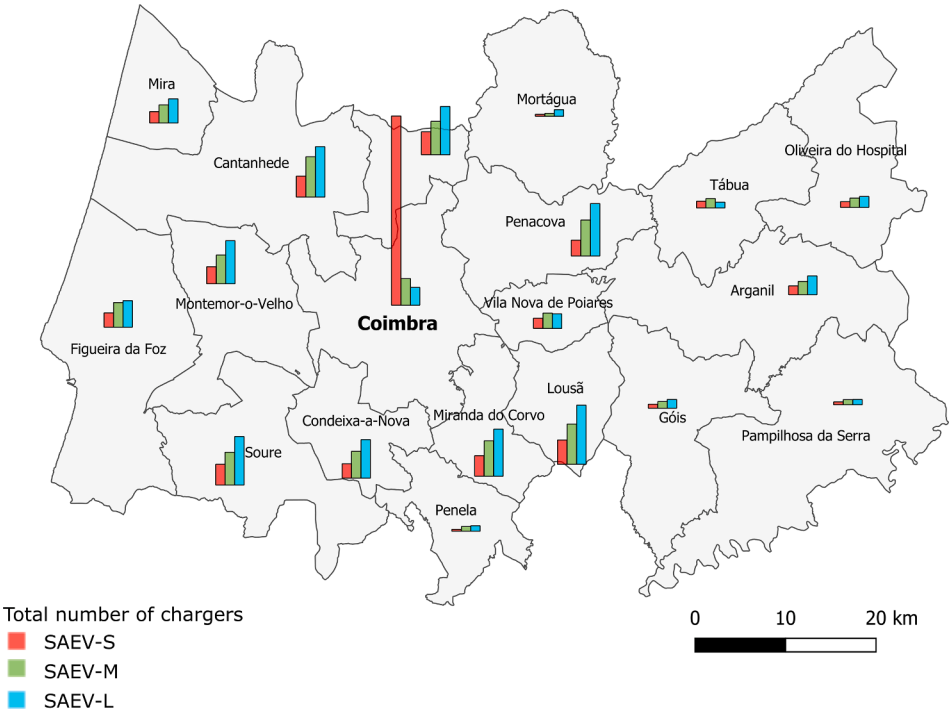

Fig. 13. Optimal geographical distribution of chargers for the scenarios with 4-seats.

Table 8
Total number of chargers per municipality for the scenarios with 4-seats.

Municipality	SAEV-S #chargers	SAEV-M #chargers	SAEV-L #chargers
Arganil	39	59	83
Cantanhede	93	178	223
Coimbra	837	118	79
Condeixa	64	119	171
Figueira da Foz	64	110	118
Góis	18	30	39
Lousã	108	178	262
Mealhada	102	148	214
Mira	50	80	107
Miranda	91	157	209
Montemor-o-Velho	76	127	191
Mortágua	9	13	29
Oliveira do Hospital	26	41	49
Pampilhosa da Serra	13	23	24
Penacova	71	160	232
Penela	8	21	24
Soure	92	145	215
Tábua	30	42	26
Vila Nova de Poiares	45	68	65

vehicles in the SAEV-L system (in blue) charge mostly during the night period, while the vehicles in the SAEV-S system (in red) charge both during the night and between demand peaks. This is justified by the analysis of the average battery SOC of the vehicles in Fig. 11. The battery of the SAEV-S vehicles (in red) decreases from an average SOC of 91% to 34%, between the beginning and the end of the morning peak. As a consequence, vehicles need to recharge again in the middle of the day, disregarding the electricity price, to sustain the second wave of demand requests in the afternoon. With the increase of vehicle range, the charging process is concentrated in the night period, though the SAEV-M system vehicles (in green) still need to have an important increment of the battery SOC during the day to ensure enough energy for the afternoon demand.

The demand peaks are coincident with the highest electricity tariff charged by the provider (see Fig. 9 and Fig. 10). This is convenient since the higher prices are naturally avoided at those intervals of time, when almost all vehicles are occupied serving trips. Indeed, all system configurations completely avoid the higher electricity tariffs in the afternoon, although in the morning some of the

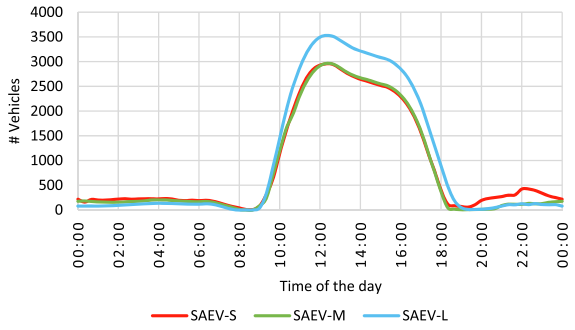

Fig. 14. Vehicles in the municipality of Coimbra for the scenarios with 4 seats.

SAEV-S system vehicles are still required to charge at the moment the price of electricity is at its maximum (see Fig. 10) which is a consequence of the vehicle battery capacity limitations.

It is interesting to see, in Fig. 9, that there is a residual amount of relocations during the day mainly due to charging operations for all SAEV configurations. Though, the number of vehicles relocating increases in waves, not only when the demand reaches its peak values (to guarantee the reposition of vehicles and serve more demand), but also right after the reduction in the electricity prices happening just before the night period (to relocate vehicles towards available charging stations). The number of idle vehicles has peaks along the day (see Fig. 9). These are related to vehicles that could be charging however due to the unattractive electricity price, opt for waiting to be used for client needs (the case of the peak observed just after 8:00 hours) or waiting for the tariff to drop (peaks observed just before 11:00 hours, and right before 21:00 hours).

The charger usage throughout the day is different between SAEV configurations (see Fig. 12). For the SAEV-L system, approximately 100% of the chargers are used during the entire night period and less than 15% during the day. On the other extreme is the SAEV-S system that uses 86% to 98% of the chargers during the day, and 54% to 78% during the night period. When 46 kW chargers are part of the system configuration, the cases of SAEV-S and SAEV-L, these chargers are used as much as possible, except when the electricity tariff is higher. It is important to note that, as shown in Figure 12, 46 kW chargers are used to quickly charge vehicles in the morning (this is consistent with the need for SAEV-S and SAEV-M vehicles to charge in the middle of the day – as shown in Fig. 11).

The different charging needs of the SAEV system, as the range of the vehicles increases, have an effect on the geographical location of the chargers. Fig. 13 and Table 8 show the total number of chargers per municipality for the optimal configurations of each vehicle range. The need to charge in the middle of the day, a characteristic of the SAEV-S configuration, leads to having vehicles charging at stations that are close to the main job and education centers of the region, located at the municipality of Coimbra (see Fig. 5). In fact, the number of vehicles of the SAEV-S system inside the municipality of Coimbra in the middle of the day reaches 2957 vehicles (see Fig. 14). This represents approximately half of the system's fleet (see Table 7). This leads to having the highest number of chargers installed in the Coimbra municipality (see Fig. 13). As the range of the vehicles increases, the charging operations occur mostly during the night period, and the location of the chargers changes to where the users live. In Fig. 13, we can see that the concentration of chargers in the Coimbra municipality, observed for the SAEV-S system, gradually changes to an evenly distributed number of chargers around the surrounding municipalities (the origins of the commuting trips), for SAEV-M and SAEV-L systems. In Fig. 14, the difference in the number of vehicles inside Coimbra during the day between SAEV-L and the other two configurations (SAEV-S and SAEV-M) is related to having fewer vehicles relocated towards the available charging stations in the surrounding municipalities. This is due to the necessity to charge during the day associated with a balanced distribution of chargers, which do not provide enough chargers inside the municipality of Coimbra and counts on these relocation movements for energy supply.

4.3. Benefits of considering a fleet with multiple vehicle types

Previously we tested systems with fleets comprised of only one vehicle type. This allowed performing a thorough analysis of the impact that different vehicle battery capacities have on system design parameters. Let's assume now that the service provider wants to design a system with a fleet comprised of multiple vehicles and needs to know how many vehicles of each type (short, medium, and long-range) lead to better profit. For this purpose, the IP model was applied to two scenarios that considers the three vehicle types (SAEV-All): one assumes that all vehicles have 1-seat capacity, and the other assumes that all vehicles have 4-seat capacity. The results are presented in Table 7.

This approach allows assessing the true optimal solution in terms of fleet size and composition. Considering a system using vehicles with 1-seat capacity, the solution of the scenario SAEV-All confirms that the optimal system design concerning the fleet is to use short-range vehicles only. We indeed obtain the same results as under the SAEV-S scenario—except for small differences in the KPIs reported in Table 7 due to negligible optimality gaps (0.04% in the SAEV-S scenario, 0.01% in the scenario SAEV-All, respectively).

For a system with 4-seats layout vehicles, the SAEV-All solution leads to higher profit than any homogenous fleet setting, unveiling business opportunities to further improve profits arising from the deployment of different vehicle types. This optimal solution is close to the SAEV-S solution, but additionally takes advantage of the use of medium-range vehicles. The resulting profit increase is equal to 203€/day (0.2%). This difference is attained from slight reductions in each cost parcel. The fleet cost of the combination of vehicles

Table 9
Sensitivity analysis results using the SAEV-S scenario with 4 seats.

	Base (SAEV-S 4-seats)	a) Equal charger cost	b) Flat tariff plan	c1) −10% demand	c2) +10% demand	c3) demand shift
Service price (€/km)	0.06	0.06	0.06	0.06	0.06	0.06
Revenue (€/day)	287,665	287,665	287,665	259,086	313,123	288,564
Total cost (€/day)	194,185	188,124	221,992	184,776	205,882	193,801
- fleet cost (€/day)	122,240	122,240	122,240	122,240	122,240	122,240
- energy cost (€/day)	63,534	62,988	93,319	54,125	75,231	63,150
- chargers cost (€/day)	8,411	2,896	6,433	8,411	8,411	8,411
Profit (€/day)	**93,480**	**99,541**	**65,673**	**74,310**	**107,241**	**94,763**
Ratio profit/revenue (%)	32%	35%	23%	29%	34%	33%
Fleet size (S range vehicles)	6,112	6,112	6,112	6,112	6,112	6,112
Total number of chargers	1,836	724	1,356	1,836	1,836	1,933
- # of 22 kW chargers	1,739	77	1,267	1,739	1,739	1,836
- # of 46 kW chargers	97	297	87	97	97	97
- # of 100 kW chargers	0	350	2	0	0	0
Total energy bought (kWh/day)	522,383	519,543	518,437	461,228	570,428	520,964
- energy moving users (kWh/day)	497,039	497,063	497,000	449,869	534,418	497,821
- relocation energy (kWh/day)	25,344	22,480	21,437	11,359	36,010	23,143
Energy bought per period:						
- empty period (%)	49.3	49.6	–	54.6	45.8	49.5
- full period (%)	49.8	49.6	–	45.3	47	49.8
- peak period (%)	0.9	0.8	–	0.1	7.2	0.7
Total trip requests/day	116,050	116,050	116,050	104,532	127,769	116,054
Total trips served/day	116,050	116,050	116,050	104,532	125,951	116,052
Total trips rejected/day	–	–	–	0	1,818	2
Trips per vehicle/day	19	19	19	17	21	19
Avg. travel time/passenger (min)*	59	59	59	59	59	58
Total # of relocations/day	5,681	5,063	4,765	2,818	7,986	5,521
Vehicle time:						
- moving users (%)	34.2	34.2	34.2	31.0	36.8	34.3
- relocation time (%)	1.7	1.6	2.0	0.8	2.5	1.6
- idle time excluding charging (%)	47.0	56.3	47.8	53.1	42.3	47.1
- charging time (%)	17.1	7.9	16.5	15.1	18.4	17.0
Vehicles moving with users:						
- avg. time/veh.mov. (min)*	94	94	94	97	96	97
- avg. # of passengers/veh.mov. (veh.mov. = vehicle movement)	3.6	3.6	3.6	3.7	3.8	3.8

* Note that discrepancies among these two values are due to the discretization adopted in the paper.

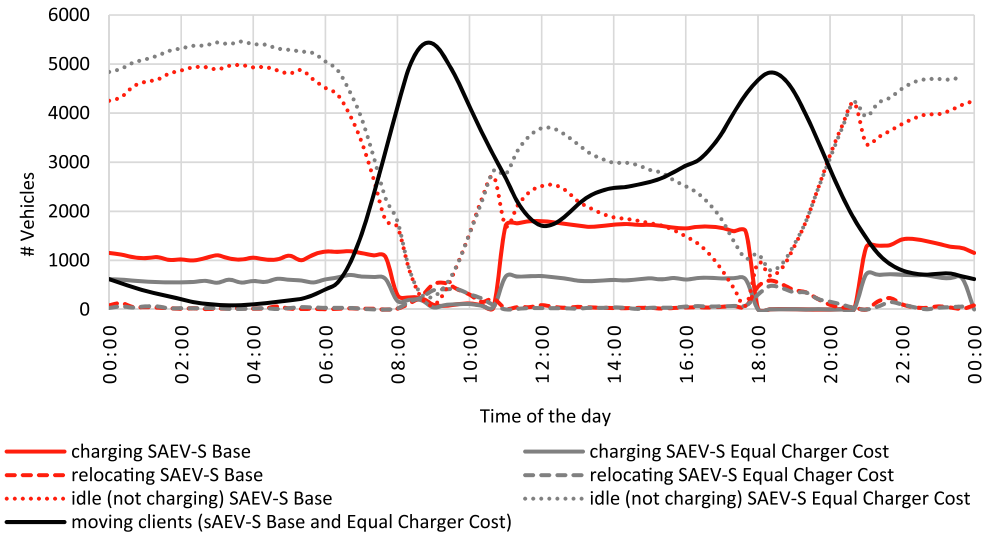

Fig. 15. State of the vehicles during the day for the base and equal charger cost scenarios.

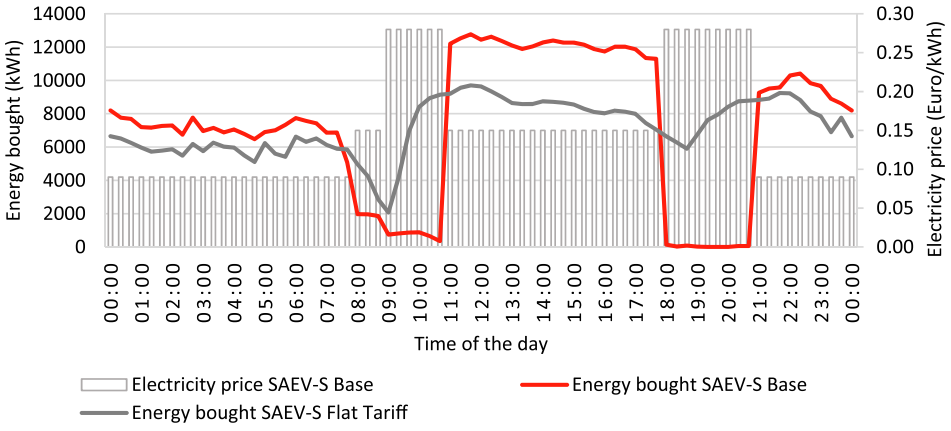

Fig. 16. Quantity of energy bought vs electricity price for the base and flat tariff scenarios.

(5,994 short-range vehicles and 77 medium-range vehicles) is lower. The vehicles consume more energy (522,789 kWh/day for the SAEV-All scenario and 522,383 kWh/day for the SAEV-S scenario), but the expense related to energy is smaller due to less energy bought during the peak period. This is attained from the different combination of chargers which includes one 100 kW charger (located in the center of the region). This combination of chargers has also lower daily installation and maintenance costs when compared to the SAEV-S optimal solution.

4.4. Sensitivity analysis

Finally, to assess the robustness of the model results, sensitivity analyses were performed on key model parameters and assumptions. In particular, we evaluate the impact of variations on the: (a) daily cost of the charging infrastructure, (b) electricity price, and (c) demand. For this assessment, we used the scenario SAEV-S with 4-seat capacity as a basis (the same scenario studied in Section 4.2).

a) daily cost of the charging infrastructure (equal chargers cost).

With the continuous upgrade of the electricity grid due to the challenges of the energy transition such as providing high power for rapid chargers and the management of intermittent power sources such as wind and solar power, it was assumed that the installation and maintenance costs for all charger types are the same and equal to 4 Euro per day. By comparing the results with the base case scenario (see Table 9), we can observe that the main changes are related to the design of the charging network. This solution (with the same cost for all charger types) includes significantly fewer slow chargers and more 100 kW chargers when compared to the base case solution. The use of faster chargers yields a 1% reduction in the total energy cost, justified by a small transfer of the amount of energy charged during the full period to the empty period (which is cheaper), and a reduction in the energy used for relocating vehicles. There is also a difference in the time that the vehicles spend charging, which is roughly half the time of the base case scenario. The less time spent charging is transferred to idle time (see Fig. 15).

b) electricity price (flat tariff plan).

The adoption of a flat rate tariff plan from the energy provider was tested as a possibility. The considered flat rate value is equal to 0.18 Euro per kWh, which is the value charged by the Portuguese company edp in their flat rate plans (edp, 2021). Fig. 16 shows the effects of the insertion of a daily flat rate. The flat tariff plan allows having a more even distribution of the energy transferred to vehicle batteries during the day. The amount of energy bought drops only during the two peak demand periods when most of the vehicles are being used to transport passengers (being more evident for the morning peak). Moreover, results in Table 9 show that a SAEV system with a flat tariff plan needs fewer chargers (a reduction of 480 chargers), and slightly less energy (a 0.8% reduction in the energy bought), which results from savings in the energy needed for relocations.

c) demand.

An additional analysis concerns the robustness and performance of the proposed system design solutions to variations in model parameters, in particular origin–destination demand estimates. Our model aims at optimizing strategic decisions underpinning the design of a SAEV system, i.e., the number and location of chargers and the number of vehicles, while accounting for vehicle flows and operations (in semi-aggregate terms) to improve considerations of vehicle and charging utilization. In practice, these decisions (system-design decisions vs. vehicle flow decisions) are characterized by different time scopes. Once the strategic decisions are made and implemented, they can hardly be adjusted on a daily basis. Instead, the optimization of vehicle flows and operations can be redone and adjusted repeatedly (subject to fleet sizing and charging infrastructure availability) to account for improved demand forecasts, or even during operations to better match the actual manifested demand. Following this logic, the robustness test was thus performed in three steps:

i. Solve the model outlined in expressions (1) to (11);
ii. Fix the strategic decisions variables, i.e., $q_{i,c}$ and v_u;

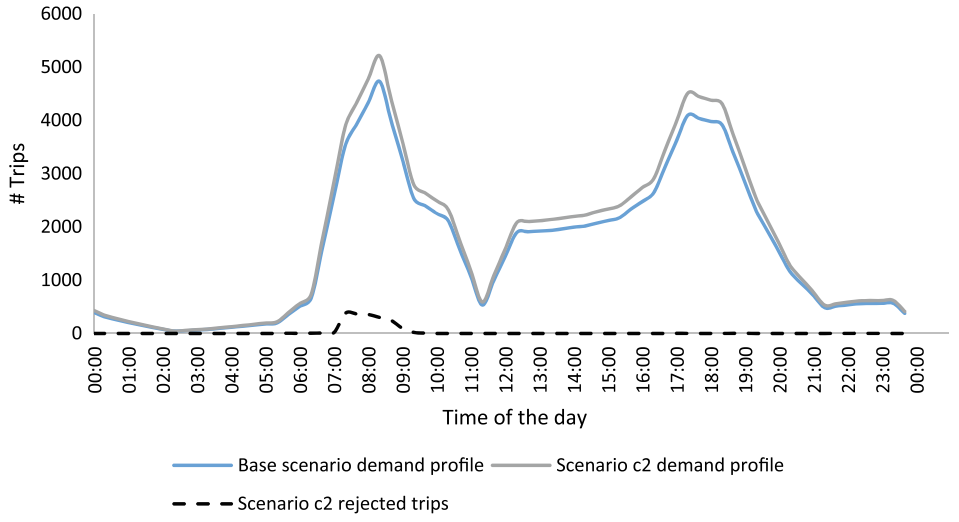

Fig. 17. Location of the rejected trips for scenario c2 (+10% demand).

iii. Consider a new demand profile ($\widetilde{D}_m$) and solve an adjusted version the optimization model (see below) wherein the strategic values are taken as fixed parameters (from step ii.) instead of decision variables.

The result is a new optimal configuration of vehicle flows for each new demand profile. It must be noted that the optimization model ran in step (iii) was altered to accommodate trip rejections, since the consideration of a given fleet and charging network, in some situations, could not be adequate to serve all demand.

The new model formulation is as follows:

$$\max(\pi) = \sum_{m\in M} p_m \times D_{m,s} - \sum_{h\in H} c_h \times y_h - \sum_{f\in F} c_f \times x_f - \sum_{c\in C}\sum_{i\in Z} c_{i,c} \times q_{i,c} - \sum_{u\in U} c_u \times v_u - \sum_{m\in M} B \times D_{m,r} \tag{12}$$

Subject to:

Expressions (2), (3), and expressions (5) to (9).

$$\widetilde{D}_m = D_{m,s} + D_{m,r},\ \forall m \in M \tag{13}$$

$$D_{m,s} \le \sum_{u\in U}\left(k_u \sum_{f\in F_{m,u}} x_f\right),\ \forall m \in M \tag{14}$$

The objective function (12) has two new decision variables $D_{m,s}$ and $D_{m,r}$ which correspond to the part of $\widetilde{D}_m$ served and rejected, respectively. The relation between these variables is defined by constraint (13). The objective function has also a new parameter B, a big value to penalize any rejected trip. Constraint (14) maintains the same function as before, though the variable D_m is now replaced by $D_{m,s}$. This new formulation allowed a relaxation of the constraints through the flexibility of trip request rejection, which is necessary to overcome the limitations of having a fixed fleet size and a fixed number of charging stations. The penalty adopted as the big value B, was set to 100 Euro for each rejected trip. Note that this value is not accounted for in the post-optimization analysis as a cost to determine the system's profit from the operator viewpoint.

Three different demand profiles were used to assess the robustness of the optimal solution (in terms of strategic system design decisions) previously obtained for the SAEV-S scenario with 4-seat capacity. Two demand profiles were randomly generated by using a reduction and increment of 10% in the hourly trip departure rates of each OD pair obtained from the mobility survey (scenarios c1 and c2). These are aimed to assess what would happen if demand is underestimated or overestimated, respectively. A third demand profile, to test the consequences of a shift of demand from the main city (Coimbra) to the remaining municipalities (scenario c3), was generated by applying a reduction of 5% to the hourly trip departure rates for each OD pair with one end in the main municipality (Coimbra), and a increment percentage of 12% to the rates of the other OD pairs. These percentages are related to each other, since they allow to have a similar number of trips reduced and incremented, resulting in approximately the same total number of trips as in the original SAEV-S scenario with 4-seat capacity. From a computational standpoint, the model remains tractable. Near optimal solutions were obtained using the software FICO Xpress with the following GAPs: 0.01%, 0.78%, and 0.37%, for scenarios c1, c2, and c3, respectively. The time limit of 10,000 seconds was turned off while using this altered model formulation, since it took longer to reach solutions with GAPs lower than 1% (from 90,000 to 300,000 seconds). Table 9 contains the optimization results.

The 10% variations in demand, scenarios c1 and c2, allowed to mark out the potential profit. A decrease of 10% in demand leads to less 20% of total profit. Despite savings in energy due to a reduction of distance covered, both with passengers and relocations, and due

Table 10
Number of decision variables for the tested network.

Decision variable sets	Number of variables	Number of variables after applying Algorithm 1
x_f	305,830,080	607,500
y_h	50,971,680	94,393
s_g	36,480	32,833
z_w	456	1905*
$q_{i,c}$	57	57
v_u	1	1
Total	356,838,754	736,689
*includes 1449 flow variables associated with compound wrap-around arcs		

Table 11
Analysis of solving times and optimization GAPs for the network problem.

Solving time in seconds	GAP values of IP model
1000	no solution
2000	11.43%
3000	0.11%
5000	0.11%
7000	0.04%
10,000	0.04%

to buying more energy at cheaper prices, the saved value, equal to 9,409 Euro, is lower than the lost revenue, which is 28,579 Euro. On the other hand, an increase of 10% in demand leads to 15% higher profit relatively to the base demand scenario. The revenue is higher by 25,458 Euro, outweighting the increase in energy cost of 11,697 Euro due to more movements, relocations, and more charging time when energy is more expensive. Additionally, the system size is not enough to accomodate all trip requests when the demand is 10% higher, leading to rejections of 1,818 trips (approximately 1% of the total requests). The rejected trips are in the morning (see Fig. 17), flattening the demand peak and making it more similar to the peak of the base scenario demand profile (the basis to design the fleet size and number of chargers).

The optimized vehicle flows in the demand shift scenario (c3) slightly increase the systems profit when compared to the base scenario (a difference of 1,283 Euro per day). Though the system size parameters that were fixed a priori (fleet and chargers) are, once more, not enough to serve all trip requests, being only two trips not served. The increase in profit is due to bigger revenues, a result of having higher total distance covered transporting passengers (an extra 15 thousand kilometers per day), and a decrease in the total energy cost. The less amount of energy bought is a result of spending less energy in relocations which overly compensates the higher amount of energy used to transport passengers.

Ultimately, this analysis has demonstrated how the proposed model can be readily used to assess reasonable variations in the model parameters to account for their uncertainties using a scenario-based approach. A more systematic capturing of these uncertainties, e.g., either through robust or stochastic optimization frameworks, can also be pursued and is left to future research.

5. Conclusions

In this study, we proposed a space–time-energy flow-based integer programming (IP) model to design a shared automated electric vehicle (SAEV) system. The concept of a three-dimensional network flow-based model was first introduced by Zhang et al. (2019) to analyze one-way carsharing movements. This work took this concept further to develop a model that performs a complete early-stage design of an SAEV system, including the fleet (size and composition), charging facilities (number and location), and vehicle operations (movements with users, relocations, and charging). The use of vehicle flows, moving through the three-dimensional network over time, allows keeping track of the location and energy of vehicles at each timestep, without greatly increasing the number of variables in the problem (as it happens when considering each vehicle individually). This simplification is possible due to the less detail needed when studying interurban movements and allows solving large-scale problems. The objective function of the problem is set to maximize the profit considering the daily fixed costs of using chargers and vehicles, as well as the costs related to the energy consumed during charging operations and the extra costs related to moving vehicles (e.g.: tolls). Charging stations with different charging power capabilities can be used in the model. An algorithm was introduced to pre-process the input data and eliminate the unnecessary arcs and nodes. This allows reducing the number of decision variables, namely the ones directly dependent on the number of arcs. It was verified that the model, after applying the pre-processing algorithm, quickly converges to close to optimal solutions (with GAP below 0.2%) in less than 10,000 seconds for problems with 19 zones, 81 timesteps, considering 3 types of chargers, 3 vehicle types, and 24 energy levels (maximum considered in the case study).

The influence of the vehicle range in the optimal design of an interurban SAEV system was assessed by applying the model to the case-study region of Coimbra (Portugal). Three different vehicle ranges were considered: short, medium, and long. Two different vehicle capacity layouts differentiate distinct services: a 1-seat layout for an experience similar to a private vehicle; and a 4-seats layout for a lower-cost service, being the trip shared with other passengers (service with pooling). Three types of chargers were available to

install in all the SAEV system configurations. The charging speed depends on the vehicles' state of charge and the energy price changes throughout the day.

The results showed that the system profit decreases with the range of the vehicles, which is mainly related to the importance of the vehicle fixed costs in the profit function. With regards to energy movements, it was observed that the adoption of long-range vehicles reduces the energy spent in relocations, and increases the energy charged during the night period at a lower price. It was observed that the charging operations naturally avoid the periods with the highest electricity tariff, benefiting from the fact that these pricey periods are coincident with the demand peaks (when most vehicles are occupied serving trips). Concerning the optimal use of chargers, the results showed that to charge more energy during the night, the long-range vehicle systems need more chargers. Though the importance of having fast chargers is reduced, since there is plenty of idle time during the night to perform the charging operations.

The optimal location of the chargers is related to the periods in which it is best to charge. Systems using short-range vehicles have more chargers close to the main commuter trip attractors (work, school, or services). On the other hand, systems with long-range vehicles have chargers located close to the afternoon trip destinations (near the homes of the users). Concerning the optimal fleet size, it was found that a lower battery capacity can lead to more vehicles in the fleet than the ones needed to serve the demand if battery capacity was not a limitation. But, the optimization process can eventually return a slightly higher number of vehicles as the range increases, if the daily cost of having a few more vehicles is lower than all the other costs combined.

The possibility of using multiple vehicle types in the fleet was tested, for the case-study conditions, considering the three vehicle types (short, medium, and long-range). The optimized solution obtained for the multiple vehicle design was similar to the one obtained for the design using only short-range vehicles. Only a very slight improvement in profit was verified. Additionally, a sensitivity analysis allowed to understand that: having the same charger daily unitary cost (installation and maintenance) result in having a higher number of fast chargers; a flat electricity tariff plan allows to have an even distribution of the energy bought during the day; and the same system size (in terms of vehicles and chargers) applied to slight demand profile changes may not be enough to serve all demand.

Lastly, the use of the presented IP model is adequate to design and assess a SAEV system for interurban traveling in an early design stage, meaning the planning stage, due to not requiring great detail on each vehicle travelers. The joint optimization of the fleet (size and composition) and chargers (number and location), in addition to vehicle movements (relocation, charging, and moving passengers), provides insights about the interaction between all these aspects, enabling a complete assessment of the optimal characteristics of such systems. The proposed model has limitations which are detailed in the model assumptions. Vehicle movements are represented by flows and the operational area zones are discretized by using centroids. This is adequate for an early design stage, though some other methodologies can be applied (e.g.: simulation) to increase the detail of the system operations, if needed, by using the model results as system design parameters. The model only considers trips between different zones, meaning that it does not include trips with origin and destination inside the same zone. The travel time in the case of vehicle pooling does not consider the number of passengers inside each vehicle, though a procedure is used to determine the approximate travel time for each origin–destination pair considering that the number of passengers picked-up and delivered is equal to vehicle seating capacity. The model considers a day of operation that repeats itself indefinitely (through the use of wrap-around arcs) without incorporating mode choice internally. The case study is a regional area with a polycentric occupation of the territory which consists of one main city that is significantly distant from other smaller cities. The presented results and conclusions about the case-study should only be transferred to similar regions.

Improvements can be added to overcome these limitations or to extend the contributions of this study, namely: add user behavior models to capture the equilibrium between demand and supply; use the intra-zone trips (urban) in addition to the inter-zonal trips, to understand how this extra usage of the vehicles during the day affects the system design; consider a time window for user departures instead of a fixed instant; take into account the traffic congestion impacts on the travel times; and consider demand stochasticity more systematically.

CRediT authorship contribution statement

Gonçalo Gonçalves Duarte Santos: Conceptualization, Methodology, Software, Validation, Formal analysis, Investigation, Data curation, Writing – original draft, Writing – review & editing. **Sebastian Birolini:** Conceptualization, Methodology, Validation, Data curation, Writing – review & editing. **Gonçalo Homem de Almeida Correia:** Conceptualization, Validation, Writing – review & editing, Supervision, Project administration, Funding acquisition.

Declaration of Competing Interest

The authors declare that they have no known competing financial interests or personal relationships that could have appeared to influence the work reported in this paper.

Acknowledgements

This work was supported by the project Driving2Driverless under the grant PTDC/ECI-TRA/31923/2017 funded by the European Regional Development Fund and by the Portuguese institution FCT (Foundation for Science and Technology). We would like to acknowledge FICO for supplying the Xpress academic license.

Appendix A. Determining travel times

Algorithm 2: processes to determine the travel times

```
Define the centroid of each zone and subzone
Store the population values for all zones and subzones
Obtain the shortest travel time between all zone centroid pairs by using real routes
Obtain the shortest travel time between all subzone centroid pairs by using real routes
Travel time with users (for arcs f ∈ F_m):
  Insert vehicle capacity k in number of seats
  For each pair of zones (i,j)
    For each experiment n = 1 to n = 100
      Generate k random pick up points at zone i in proportion with the population weight of each subzone in all subzones of i; Do the same for zone j
      Use simulated annealing to determine the shortest distance between all generated points
      Store the shortest distance travel time value
    End For
    Determine the average of all stored shortest distance travel time values → travel time value (i,j)
  End For
Relocation travel time (for arcs f ∈ F ∧ f ∉ F_m):
  For each pair of zones (i,j)
    The shortest travel time between centroids of the pair of zones → travel time value (i,j)
  End For
```

Distinct processes are used to determine the travel times for vehicles moving with users, and vehicles relocating (see Algorithm 2). The travel time of vehicles with users between a certain origin–destination pair is determined using a Monte Carlo technique with n experiments to create a sample. For each experiment, it was assumed that the number of passenger pick-ups at the zone of origin, as well as the number of drop-offs at the destination zone, is equal to the vehicle capacity. This is necessary because the optimization model, which describes vehicle flows, does not know how many users travel inside each vehicle. This way, the resulting travel time value is valid, on the safe side, for all possible occupancy rates. Zones are divided into subzones to increase realism (see Fig. 1). Each subzone is represented by a spatial node. Pick-up points and drop-off locations are generated using the inverse transform sampling method applied using the population weight of each subzone in the origin and destination zones, respectively. The shortest distance between all pick-up points and drop-off locations is determined using a simulated annealing algorithm (Eglese, 1990), which is normally used to solve traveling salesman problems such as this one (without return to the starting point). The distances between all sub-zones are needed to run this metaheuristic. The travel time for vehicles with users results from the average value of the obtained sample. In contrast, the travel time of vehicles relocating corresponds simply to the shortest distance between the representative nodes of origin and destination zones (see Fig. 1).

Appendix B. Computational speed assessment

An assessment of the computational speed was performed using a network similar to the one used for the SAEV-L scenario (presented in this work). The network has 19 zones, 81 timesteps, 24 energy levels (considering that the energy does not drop below level 1), includes 3 charger types, and only one vehicle type. The referred number of timesteps correspond to 72 timesteps of 20 minutes, plus additional timesteps for vehicle moving activities that extend beyond the 24-hour period. The network was loaded with 116 thousand demand requests. The charging speed was considered to vary with the battery SOC, being the charging curves different for each charger type. In addition, it was considered that each car spends one energy level to move during one timestep. Algorithm 1 was applied to define only the needed arcs and nodes, reducing the total number of decision variables by approximately 480 times (see Table 10).

This early assessment allowed us to understand the solving efficiency when using the FICO Xpress solver applied to the network generated by Algorithm 1. The results obtained are presented in Table 11. The same desktop computer as described in Section 4 (with an Intel Core i7-8700 processor with 3.20 GHz processing speed, a Solid-State Drive, and 16 GB of RAM) was used in this process. A time limit of 10 thousand seconds was set to find an optimal solution. It was found that the model converges to a GAP below 1% in less than one hour.

References

Amr, 2021. Robo taxi market [WWW Document]. accessed 4.19.22. https://www.alliedmarketresearch.com/robo-taxi-market.

Bernhart, W., Kaise, H., Ohashi, Y., Schönberg, T., Schilles, L., 2018. Autonomous driving as a solution for non-urban mobility Management summary. Rol. Berger Focus.

Bierlaire, M., 2015. Simulation and optimization: A short review. Transp. Res. Part C Emerg. Technol. 55, 4–13. https://doi.org/10.1016/j.trc.2015.01.004.

Birolini, S., Antunes, A.P., Cattaneo, M., Malighetti, P., Paleari, S., 2021. Integrated flight scheduling and fleet assignment with improved supply-demand interactions. Transp. Res. Part B Methodol. 149, 162–180. https://doi.org/10.1016/j.trb.2021.05.001.

Carolina, N., 2020. Autonomous Vehicles in the US : 50-State Roundup US Road to Autonomy 2020 Recap.

Chen, T., Zhang, B., Pourbabak, H., Kavousi-Fard, A., Su, W., 2018. Optimal Routing and Charging of an Electric Vehicle Fleet for High-Efficiency Dynamic Transit Systems. IEEE Trans. Smart Grid 9, 3563–3572. https://doi.org/10.1109/TSG.2016.2635025.

Chen, T.D., Kockelman, K.M., Hanna, J.P., 2016. Operations of a shared, autonomous, electric vehicle fleet: Implications of vehicle & charging infrastructure decisions. Transp. Res. Part A Policy Pract. 94, 243–254. https://doi.org/10.1016/j.tra.2016.08.020.

Dong, Z., Chuhang, Y., Lau, H.Y.K.H., 2016. An integrated flight scheduling and fleet assignment method based on a discrete choice model. Comput. Ind. Eng. 98, 195–210. https://doi.org/10.1016/j.cie.2016.05.040.
Drews, F., Luxen, D., 2013. Multi-hop ride sharing. Proc. 6th Annu. Symp. Comb. Search, SoCS 2013, 71–79.
edp, 2021. Tarifários [WWW Document]. URL https://www.edp.pt/particulares/energia/tarifarios/ (accessed 1.20.21).
Eglese, R.W., 1990. Simulated annealing: A tool for operational research. Eur. J. Oper. Res. 46, 271–281. https://doi.org/10.1016/0377-2217(90)90001-R.
ev-database, 2021. Electric Vehicle Database [WWW Document]. URL https://ev-database.org/ (accessed 2.1.20).
Ewing, J., 2021. How Germany hopes to get the edge in driverless technology [WWW Document]. New York Times. URL https://www.nytimes.com/2021/07/14/business/germany-autonomous-driving-new-law.html (accessed 4.19.22).
Farhan, J., Chen, D., 2018. Impact of Ridesharing on Operational Efficiency of Shared Autonomous Electric Vehicle Fleet. Transp. Res. Part C Emerg. Technol. 93, 310–321.
Fastned, 2021. Vehicles & charging tips [WWW Document]. URL https://fastnedcharging.com/en/ (accessed 2.1.20).
Google, 2019. Google Maps [WWW Document]. URL https://www.google.pt/maps/ (accessed 12.18.19).
Hao, X., Zhou, Y., Wang, H., Ouyang, M., 2020. Plug-in electric vehicles in China and the USA: a technology and market comparison. Mitig. Adapt. Strateg. Glob. Chang. 25, 329–353. https://doi.org/10.1007/s11027-019-09907-z.
Huang, K., An, K., Correia, G.H. de A., 2020. Planning station capacity and fleet size of one-way electric carsharing systems with continuous state of charge functions. Eur. J. Oper. Res. 287, 1075–1091. https://doi.org/10.1016/j.ejor.2020.05.001.
Iacobucci, R., McLellan, B., Tezuka, T., 2019. Optimization of shared autonomous electric vehicles operations with charge scheduling and vehicle-to-grid. Transp. Res. Part C Emerg. Technol. 100, 34–52. https://doi.org/10.1016/j.trc.2019.01.011.
Iacobucci, R., McLellan, B., Tezuka, T., 2018. Modeling shared autonomous electric vehicles: Potential for transport and power grid integration. Energy 158, 148–163. https://doi.org/10.1016/j.energy.2018.06.024.
Iglesias, R., Rossi, F., Wang, K., Hallac, D., Leskovec, J., Pavone, M., 2018. Data-driven model predictive control of autonomous mobility-on-demand systems. Proc. - IEEE Int. Conf. Robot. Autom. 6019–6025 https://doi.org/10.1109/ICRA.2018.8460966.
Imhof, S., Frölicher, J., von Arx, W., 2020. Shared Autonomous Vehicles in rural public transportation systems. Res. Transp. Econ. 83, 1–7. https://doi.org/10.1016/j.retrec.2020.100925.
INE, 2011. População residente e densidade populacional por local de residência; Anual - INE, Estimativas anuais da população residente [WWW Document]. accessed 12.12.19. https://censos.ine.pt/xportal/xmain?xpid=CENSOS&xpgid=censos2011_apresentacao.
Jamshidi, H., Correia, G.H.A., van Essen, J.T., Nökel, K., 2021. Dynamic planning for simultaneous recharging and relocation of shared electric taxies: A sequential MILP approach. Transp. Res. Part C Emerg. Technol. 125, 102933 https://doi.org/10.1016/j.trc.2020.102933.
Liang, X., Correia, G.H. de A., van Arem, B., 2016. Optimizing the service area and trip selection of an electric automated taxi system used for the last mile of train trips. Transp. Res. Part E Logist. Transp. Rev. 93, 115–129. https://doi.org/10.1016/j.tre.2016.05.006.
Martinez, L.M., Correia, G.H.A., Viegas, J.M., 2015. An agent-based simulation model to assess the impacts of introducing a shared-taxi system: an application to Lisbon (Portugal). J. Adv. Transp. 49, 475–495. https://doi.org/10.1002/atr.1283.
Nieuwenhuijsen, J., Correia, G.H. de A., Milakis, D., van Arem, B., van Daalen, E., 2018. Towards a quantitative method to analyze the long-term innovation diffusion of automated vehicles technology using system dynamics. Transp. Res. Part C Emerg. Technol. 86, 300–327. https://doi.org/10.1016/j.trc.2017.11.016.
Pacheco Paneque, M., Bierlaire, M., Gendron, B., Sharif Azadeh, S., 2021. Integrating advanced discrete choice models in mixed integer linear optimization. Transp. Res. Part B Methodol. 146, 26–49. https://doi.org/10.1016/j.trb.2021.02.003.
Santos, G.G.D., Correia, G.H. de A., 2021. A flow-based integer programming approach to design an interurban shared automated vehicle system and assess its financial viability. Transp. Res. Part C Emerg. Technol. 128, 103092. https://doi.org/10.1016/j.trc.2021.103092.
Scheltes, A., de Almeida Correia, G.H., 2017. Exploring the use of automated vehicles as last mile connection of train trips through an agent-based simulation model: An application to Delft. Netherlands. Int. J. Transp. Sci. Technol. 6, 28–41. https://doi.org/10.1016/j.ijtst.2017.05.004.
Sherali, H.D., Bish, E.K., Zhu, X., 2006. Airline fleet assignment concepts, models, and algorithms. Eur. J. Oper. Res. 172, 1–30. https://doi.org/10.1016/j.ejor.2005.01.056.
Smith, M., Castellano, J., 2015. Costs Associated With Non-Residential Electric Vehicle Supply Equipment. U.S. Dep. Energy 1–43.
Stevens, M., Correia, G.H. de A., Scheltes, A., van Arem, B., 2022. An agent-based model for assessing the financial viability of autonomous mobility on-demand systems used as first and last-mile of public transport trips: A case-study in Rotterdam, the Netherlands. Res. Transp. Bus. Manag. 100875. https://doi.org/10.1016/j.rtbm.2022.100875.
Taiebat, M., Xu, M., 2019. Synergies of four emerging technologies for accelerated adoption of electric vehicles: Shared mobility, wireless charging, vehicle-to-grid, and vehicle automation. J. Clean. Prod. 230, 794–797. https://doi.org/10.1016/j.jclepro.2019.05.142.
TheAA.com, 2019. Car depreciation | AA [WWW Document]. URL https://www.theaa.com/car-buying/depreciation (accessed 12.21.19).
TIS.pt, 2009. Inquérito à mobilidade na área de influência do sistema de mobilidade do Mondego, Coimbra.
Tsao, M., Iglesias, R., Pavone, M., 2018. Stochastic Model Predictive Control for Autonomous Mobility on Demand. IEEE Conf. Intell. Transp. Syst. Proceedings, ITSC 2018-Novem, 3941–3948. https://doi.org/10.1109/ITSC.2018.8569459.
ViaMichelin, 2021. ViaMichelin [WWW Document]. URL https://www.viamichelin.pt/ (accessed 4.2.21).
Waymo, 2022. Waymo one [WWW Document]. URL https://waymo.com/waymo-one/ (accessed 4.19.22).
Wen, J., Zhao, D., Zhang, C., 2020. An overview of electricity powered vehicles: Lithium-ion battery energy storage density and energy conversion efficiency. Renew. Energy 162, 1629–1648. https://doi.org/10.1016/j.renene.2020.09.055.
Winter, K., Cats, O., Correia, G.H. de A., van Arem, B., 2016. Designing an Automated Demand-Responsive Transport System: Fleet Size and Performance Analysis for a Campus–Train Station Service. Transp. Res. Rec. J. Transp. Res. Board 2542, 75–83. https://doi.org/10.3141/2542-09.
Zhang, D., Liu, Y., He, S., 2019. Vehicle assignment and relays for one-way electric car-sharing systems. Transp. Res. Part B Methodol. 120, 125–146. https://doi.org/10.1016/j.trb.2018.12.004.
Zhang, R., Rossi, F., Pavone, M., 2016. Model predictive control of autonomous mobility-on-demand systems. Proc. - IEEE Int. Conf. Robot. Autom. 2016-June, 1382–1389. https://doi.org/10.1109/ICRA.2016.7487272.